

西大别山早白垩世谭冲和陈冲花岗岩体 U-Pb 年龄、 地球化学和 Sr-Nd-Hf 同位素特征： 对岩石成因和下地壳拆沉时限的约束

朱江^{1, 2)}, 吴昌雄³⁾, 彭三国^{1, 2)}, 刘锦明³⁾, 张闯³⁾, 陈祺⁴⁾

1) 中国地质调查局武汉地质调查中心, 武汉, 430205;

2) 中国地质调查局花岗岩成岩成矿地质研究中心, 武汉, 430205;

3) 湖北省地质局第六地质大队, 湖北孝感, 432000; 4) 中国地质大学(武汉), 武汉, 430074

内容提要:谭冲和陈冲岩体出露于西大别造山带新县岩基北缘, 主要岩性分别为二长花岗岩和花岗斑岩。为理解其岩石成因和构造属性, 对两个岩体开展了激光等离子质谱(LA-ICP-MS)锆石 U-Pb 测年、元素地球化学和 Sr-Nd-Hf 同位素研究。结果表明, 谭冲和陈冲岩体锆石 U-Pb 年龄分别为 133.5 ± 1.1 Ma(MSDW=0.63) 和 132.9 ± 1.1 Ma(MSDW=1.30), 暗示其形成于早白垩世。岩石均具有较高的 SiO_2 (69.40%~77.82%)、 Al_2O_3 (11.72%~15.26%) 和总碱($\text{Na}_2\text{O} + \text{K}_2\text{O}$ =6.40%~8.70%)含量, $\text{K}_2\text{O}/\text{Na}_2\text{O}$ 比值大于 1, 过铝质(A/CNK =1.14~1.66, 一个样品值 0.97 除外)等特点, 总体归为高钾钙碱性系列。岩石富集轻稀土($(\text{La/Yb})_N$ =22.98~28.64), 负 Eu 异常不明显, 亏损 Ba、Nb、Ta、P、Ti 和 Y 元素。岩石锶同位素初始比值 I_{Sr} 为 $0.707220 \sim 0.707557$, 钫同位素 $\epsilon_{\text{Nd}}(t)$ 值为 $-17.7 \sim -18.1$, 两阶段 Nd 模式年龄 T_{DM2} = $2.36 \sim 2.40$ Ga。锆石 $\epsilon_{\text{Hf}}(t)$ 值集中于 $-21.4 \sim -25.8$, 两阶段 Hf 模式年龄 T_{DM2} = $2.24 \sim 2.48$ Ga。详细的矿物组成、岩石地球化学和 Sr-Nd-Hf 同位素分析揭示, 两个岩体成因类型均为分异的 I 型花岗岩, 起源于残留相含有石榴子石的部分熔融岩浆。岩浆房形成压力和深度较大, 可能是在加厚下地壳环境扬子陆块北缘古老陆壳物质重熔的产物。结合区域同期岩浆岩对比研究认为, 西大别地区与东大别地区加厚下地壳拆沉时限基本一致, 发生在 133 Ma 左右。

关键词:花岗岩; 地质年代学; 地球化学; Sr-Nd-Hf 同位素; 岩石成因; 西大别山

大别山造山带属于秦岭造山带东延部分, 为三叠纪扬子陆块俯冲于华北陆块之下形成的大陆碰撞造山带, 在晚中生代又经历了加厚下地壳拆沉(Ma Changqian et al., 1998; Jahn et al., 1999; Gao Shan et al., 1999; Xu Haijin et al., 2007, 2013; Zhang Chao et al., 2008; Chen Ling et al., 2012; Chen Wei et al., 2013a; Xu Yixian et al., 2016)。区域内白垩纪中酸性岩浆活动强烈, 出露面积约占全区 47%(Ratschbacher et al., 2003)。老湾金矿床(Yang Meizhen et al., 2014)、皇城山银矿床(Yang Meizhen et al., 2011; Zhu Jiang et al., 2018a)、千鹅冲钼矿床(Yang Meizhen et al., 2010;

Gao Yang et al., 2014)、沙坪沟钼矿床(Ren Zhi et al., 2014)等大型或超大型矿床均与白垩纪中酸性岩浆作用关系密切。因此, 晚中生代强烈岩浆活动记录了相关构造环境、不同热源和物源对花岗岩浆作用的贡献(Wang Chao et al., 2010; Gao Xinyu et al., 2013), 进而可能借此窥视大别山晚中生代动力学演化与大规模成矿。

以商麻断裂为界, 大别造山带可分为西大别和东大别地区。前人对东大别(商麻断裂以东)白垩纪岩浆活动开展了大量研究, 多认为其下地壳拆沉作用发生在 132 Ma 左右(Xu Shutong et al., 1992; Ma Changqian et al., 1998; Jahn et al., 1999;

注:本文为中国地质调查局地质调查项目(编号 DD20160030)资助成果。

收稿日期:2018-05-28; 改回日期:2018-10-24; 网络发表日期:2018-11-30; 责任编辑:周健。

作者简介:朱江,男,1985 年生。博士,高级工程师,主要从事矿产普查与勘探研究。Email:zhujiang_01@foxmail.com。

引用本文:朱江, 吴昌雄, 彭三国, 刘锦明, 张闯, 陈祺. 2019. 西大别山早白垩世谭冲和陈冲花岗岩体 U-Pb 年龄、地球化学和 Sr-Nd-Hf 同位素特征:对岩石成因和下地壳拆沉时限的约束. 地质学报, 93(7): 1671~1686, doi: 10.19762/j.cnki.dzjx.2019054.

Zhu Jiang, Wu Cangxiong, Peng Sanguo, Liu Jinming, Zhang Chuang, Chen Qi. 2019. U-Pb zircon age, geochemistry and isotopic characteristics of the Tanchong and Chenchong granites in the western Dabie orogen, China: constraints on petrogenesis and timing of lower crustal delamination. Acta Geologica Sinica, 93(7): 1671~1686.

Zhao Zifu et al., 2005, 2007, 2008, 2009; Huang et al., 2007; Xu Haijin et al., 2007, 2013; Chen Ling et al., 2009; Xu Yixian et al., 2016)。但迄今西大别地区白垩纪岩浆岩的岩石学、地球化学和年代学研究仍相对薄弱,远不及东大别地区研究程度(Chen Wei et al., 2013a, 2016; Gao Xinyu et al., 2013)。区内对三个大岩基(新县岩基、灵山岩基、夏店岩基)和若干与成矿关系密切的岩体(如姚冲、宝安寨、大银尖岩体等)开展了年代学和岩石地球化学研究(Zhou Hongsheng et al., 2009; Li Hongchao et al., 2012; Chen Wei et al., 2013a, 2013b, 2015; Gao Xinyu et al., 2013; Meng Fang, 2013; Wan Jun et al., 2017)。且已有研究对西大别地区白垩纪下地壳拆沉时限尚存在不同认识(Ma Changqian et al., 2003; Wang Chao et al., 2010; Gao Yang et al., 2014; Chen Wei et al., 2015),如:Gao Xinyu et al.(2013)基于商城和达权店岩体对比,认为大别地区构造体制转换的最长时间为 137 ± 2 Ma;Chen Wei et al. (2015)认为姚冲岩体(133 ± 1 Ma)形成于加厚地壳背景,暗示拆沉作用不早于133Ma;Gao Yang et al. (2014)提出千鹅冲斑岩型钼矿床形成于130Ma左右,此时矿区之下的加厚下地壳可能局部尚未拆沉。综上,东、西大别山白垩纪构造拆沉时限及动力学演化是否存在差异?这一问题仍有待于西大别岩浆岩的进一步研究。

谭冲和陈冲岩体出露于西大别造山带新县岩基北缘,研究程度较低,迄今尚无可靠年代学数据和成因研究报道。本文通过系统的锆石U-Pb年代学、岩石地球化学和Sr-Nd-Hf同位素分析,探讨这两个岩体成因和成岩环境,为理解大别山地区白垩纪构造-岩浆演化过程和下地壳拆沉时限提供更多约束。

1 地质背景

大别造山带属东秦岭造山带的东延部分,为华北和扬子两大板块拼合部位。由太古宙至早中生代,该区域经历了多期次、多阶段的碰撞—扩张—聚合的演化过程(Zhang Guowei et al., 2001; Wu Yuanbao et al., 2013)。新元古代晚期—早中生代初期板块俯冲—碰撞的构造体制造就了桐柏—大别造山带的基本构造格局(Zhang Guowei et al., 2001)。三叠纪后,华北和华南板块拼合,桐柏—大别造山带进入陆内演化阶段(Zhang Guowei et al., 2001; Wu Yuanbao et al., 2013)。早白垩世受环

太平洋构造域的影响,中国中东部进入以NNE至近SN向构造为主、近EW向构造为次的动力体制大转换时期(Ren Jishun et al., 1990)。大别山地区在早—中白垩世先后发生了地壳加厚、下地壳拆沉、大规模幔源岩浆上涌和地壳强烈伸展,诱发了大规模的岩浆活动和强烈的成矿作用(Zhang Chao et al., 2008; Chen Wei et al., 2013a; Liu Huan et al., 2019)。以商麻断裂为界,大别造山带分为西大别和东大别地区。

西大别地区在形状上呈一个楔形体,以商麻断裂为东界,以新黄断裂为西界。根据变质程度及原岩特征,该区由北向南被划分为六个岩石构造单元(图1):南湾复理石带(南湾组)、肖家庙混杂岩带、浒湾高压带(浒湾岩组)、新县超高压带、红安高压带(红安岩群)和木兰山蓝片岩-绿片岩带(Liu Xiaochun et al., 2004)。不同构造单元岩石组合和变质特征详见Liu Xiaochun et al.(2004)。区域主要岩石类型有构造片岩、片麻岩、花岗质片麻岩片麻状花岗岩、榴辉岩、角闪岩、混合岩以及糜棱岩等。区内各个地质时期均有不同程度的岩浆活动,并以新元古代和白垩纪中酸性侵入岩最为发育。白垩纪规模巨大的花岗岩基主要有灵山岩基、新县岩基和夏店岩基等(Zhou Hongsheng et al., 2009; Chen Wei et al., 2013a, 2017; Meng Fang, 2013; Wan Jun et al., 2017);大量小规模花岗岩侵入体出露广泛,与成矿关系密切(如姚冲、肖畈、母山、千鹅冲、老湾岩体等,Xu Changhai et al., 1998; Liu Yifei et al., 2008; Gao Yang et al., 2014; Chen Wei et al., 2015; Yang Zeqiang et al., 2015; Yang Yongfei et al., 2017)。区内白垩纪火山活动亦比较强烈,主要发育陈棚组中酸性火山岩,呈孤岛状零星出露于信阳市罗山县仙桥、光山县泼陂河一带(Du Jianguo et al., 1999; Ding Li et al., 2006; Yang Meizhen et al., 2012; Zhu Jiang et al., 2018a)。

2 岩石学特征

谭冲和陈冲岩体出露于新县岩体以北的新县浒湾—泼陂河镇附近(图2)。谭冲岩体出露面积约7km²,侵位于浒湾岩组和肖家庙岩组中。岩体长轴呈近NNW向,主要岩性为中细粒二长花岗岩。岩石呈淡红色,中细粒花岗结构,块状构造。主要矿物为钾长石35%~40%(微斜长石和条纹长石)、斜长石30%~35%、石英25%~30%和黑云母2%~

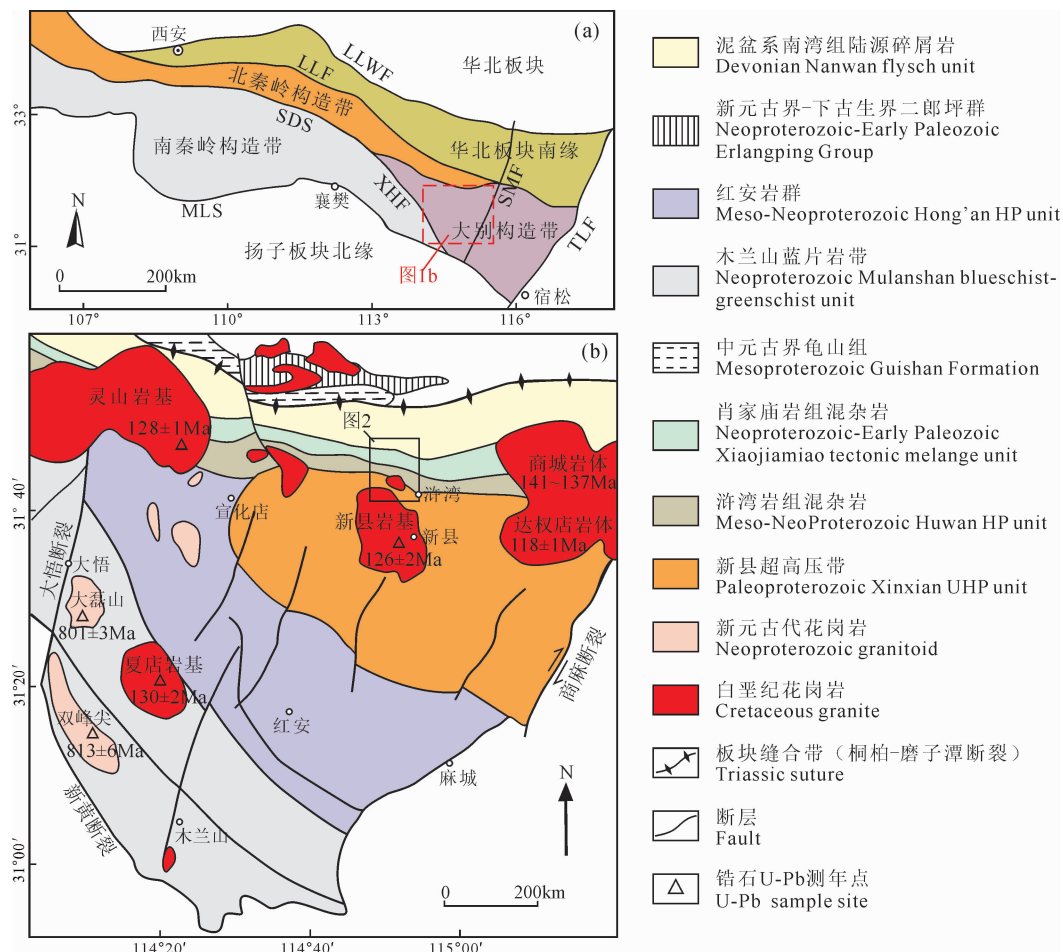


图 1 西大别地区大地构造位置图(a)和区域地质简图(b)(据 Liu Xiaochun et al., 2004 修改)

Fig. 1 The location (a) and geological sketch map (b) of the western Dabie belt (modified from Liu Xiaochun et al., 2004)

LLWF—灵宝-鲁山-舞阳断裂; LLF—洛南-栾川断裂; SDS—商县-丹凤-桐柏构造带; MLS—勉略构造带; XHF—新黄断裂; SMF—商麻断裂; TLF—郯庐断裂; 岩体 U-Pb 同位素年龄据 Liu Xiaochun et al., 2005; Zhou Hongsheng et al., 2009; Chen Wei et al., 2013; Gao Xinyu et al., 2013; Meng Fang, 2013; Cao Zhenqi et al., 2017; Wan Jun et al., 2017; Wu Yudong et al., 2017

LLWF—Lingbao-Lushan-Wuyang fault; LLF—Luonan-Luanchuan fault; SDS—Shangdan-Tongshang suture; MLS—Mianlue suture; XHF—Xinhuang fault; SMF—Shangma fault; TLF—Tanlu fault. The ages of granites are from Liu Xiaochun et al., 2005; Zhou Hongsheng et al., 2009; Chen Wei et al., 2013a; Gao Xinyu et al., 2013; Meng Fang, 2013; Cao Zhengqi et al., 2017; Wan Jun et al., 2017; Wu Yudong et al., 2017

3% (图 3)。副矿物有磷灰石、磁铁矿、锆石、榍石、褐帘石和金红石等。

陈冲岩体出露面积约 6 km^2 , 长轴为 NNW 向, 边部产有蟹爪状近东西向岩枝。主要岩性为花岗斑岩。岩石呈淡红色或灰白色, 斑状结构, 块状构造。斑晶含量约 20%~40%, 粒径 0.1~2mm, 主要为钾长石 3%~5%、斜长石 5%~26%、石英 5%~8% 和黑云母 1%~2%。基质含量约 60%~80%, 主要为钾长石 40%、斜长石 10% 和石英 20%。副矿物有磷灰石、磁铁矿、锆石和榍石等。

3 样品和分析方法

样品采自公路两侧或采石场的地表新鲜露头,

采样点散布于整个岩体出露区域。谭冲和陈冲岩体分别各选取了 1 件代表性样品进行锆石 U-Pb 年龄和 Lu-Hf 同位素分析, 7 件样品磨成 200 目以下粉末用于主、微量元素分析, 4 件样品用于 Sr-Nd 同位素组成分析。

3.1 锆石 U-Pb 同位素测定

锆石分选在广州拓岩分析技术有限公司完成, 原岩样品经常规破碎、磁选和重选, 得到纯度较高的锆石, 然后在双目镜下经人工挑选出纯度在 99% 以上的锆石。在双目镜下对锆石进行分类, 挑选晶形完好、未蚀变的锆石颗粒制成样品靶, 对锆石进行了透射光、反射光和阴极发光照相。选择样品靶中环带结构发育较好、裂隙较少的锆石, 采用 LA-ICP-

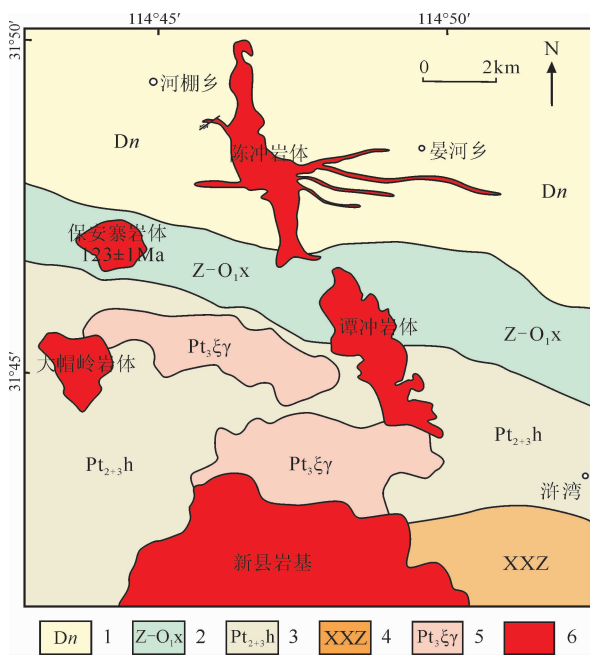


图 2 谭冲和陈冲岩体地质图

Fig. 2 Geological map of the Tanchong and Chenchong stocks

1—泥盆系南湾组陆源碎屑岩;2—肖家庙岩组混杂岩;3—浒湾岩组混杂岩;4—新县超高压带;5—新元古代花岗岩;6—白垩纪花岗岩
1—Devonian Nanwan Formation flysch unit; 2—Xiaojiamiao tectonic melange unit; 3—Meso-Neoproterozoic Huwan unit; 4—Xinxian ultrahigh-pressure unit; 5—Neoproterozoic granitoid; 6—Cretaceous granite

MS 技术进行 U-Pb 同位素测定。可见光显微照片和阴极发光图像在武汉上谱分析科技有限责任公司完成, 镐石 U-Pb 同位素组成和微量元素含量在该公司实验室利用 LA-ICP-MS 同时分析完成。激光剥蚀系统为 GeoLas 2005, ICP-MS 质谱仪为 Agilent 7500a。本次测试中采用的激光剥蚀束斑直径为 $32 \mu\text{m}$, 能量密度为 10 J/cm^2 。激光剥蚀过程中采用氦气作载气、氩气为补偿气以调节灵敏度, 二者在进入 ICP 之前通过一个 T 型接头混合。在等离子体中心气流($\text{Ar} + \text{He}$)中加入了少量氮气, 以提高仪器灵敏度、降低检出限和改善分析精密度(Hu Zhaochu et al., 2008)。另外, 激光剥蚀系统配置了一个信号平滑装置(Hu Zhaochu et al., 2012b)。每个时间分辨分析数据包括大约 $20 \sim 30 \text{ s}$ 的空白信号和 50 s 的样品信号。U-Pb 同位素定年中采用锆石标准 91500 作外标进行同位素分馏校正, 每分析 5 个样品点, 分析 2 次 91500。对于与分析时间有关的 U-Th-Pb 同位素比值漂移, 利用 91500 的变化采用线性内插的方式进行了校正(Liu Yongsheng et al., 2010)。

锆石标准 91500 的 U-Th-Pb 同位素比值推荐值据 Wiedenbeck et al. (1995)。详细的仪器操作条件和数据处理方法同文献 Liu et al. (2008, 2010)。对分析数据的离线处理(包括对样品和空白信号的选择、仪器灵敏度漂移校正、元素含量及 U-Th-Pb 同位素比值和年龄计算)采用软件 ICPMSDataCal (Liu Yongsheng et al., 2008, 2010) 完成, 所给定的同位素比值和年龄的误差(标准偏差)在 1σ 水平。锆石 U-Pb 年龄谐和图绘制和年龄加权平均计算均利用 Isoplot (Ludwig, 2003) 完成。

3.2 全岩地球化学分析

选取新鲜、未蚀变的岩石样品, 破碎至 200 目后, 进行全岩主量元素和微量、稀土元素测试。测试分析在中国地质调查局武汉地质调查中心完成, 主量元素分析仪器为荷兰 PW2440 型波长色散 X 荧光光谱仪, 分析精度优于 3.2%。微量和稀土元素分析仪器为美国等离子质谱仪和法国 JY38S 型等离子体原子发射光谱仪, 分析精度优于 4%。

3.3 全岩 Sr-Nd 同位素分析

样品制备在中国地质调查局武汉地质调查中心进行, 采用常规离子交换树脂技术进行样品分离。在该单位同位素实验室德国 Finnigan 公司 MAT-261 热电离蒸发固体质谱计(TIMS)上测定 Sr、Nd 同位素。用 NBS987 和 GBW04419 标准物质对仪器和分析流程进行监控。 $^{87}\text{Rb}/^{86}\text{Sr}$ 和 $^{147}\text{Sm}/^{144}\text{Nd}$ 比值由测得的 Rb、Sr、Sm、Nd 含量计算得出。Sr 和 Nd 同位素的分馏校正分别采用 $^{86}\text{Sr}/^{88}\text{Sr} = 0.1194$ 和 $^{146}\text{Nd}/^{144}\text{Nd} = 0.7219$ 。测试期间, NBS987 标准给出的 $^{87}\text{Sr}/^{86}\text{Sr}$ 平均值为 0.71034 ± 26 (2σ), GBW04419 标准给出的 $^{143}\text{Nd}/^{144}\text{Nd}$ 平均值为 0.512725 ± 7 (2σ)。全程 Sr 空白 $< 4 \text{ ng}$, Nd 空白 $< 1 \text{ ng}$ 。详细分析方法见 Zhu Jiang et al. (2017)。

3.4 锆石 Lu-Hf 同位素测定

锆石 Lu-Hf 同位素分析在中国地质大学(武汉)地质过程与矿产资源国家重点实验室 Neptune 多接收 MC-ICP-MS 配套的 GeoLas 2005 剥蚀系统上进行。激光剥蚀所用斑束直径为 $44 \mu\text{m}$, 能量为 5.3 J/cm^2 , 剥蚀过程中氦气作载气, 详细仪器条件和数据获取详见 Hu Zhaochu et al. (2012b)。为了校正 ^{176}Lu 和 ^{176}Yb 对 ^{176}Hf 的干扰, 取 $^{176}\text{Lu}/^{175}\text{Hf} = 0.02656$ 和 $^{176}\text{Yb}/^{173}\text{Yb} = 0.79381$ (Blichert-Toft et al., 1997) 为定值。采用 $^{173}\text{Yb}/^{171}\text{Yb} = 1.1248$ 和 $^{179}\text{Hf}/^{177}\text{Hf} = 0.7325$ 分别对 Yb 同位素和 Hf 同位素



图 3 谭冲和陈冲岩体手标本和显微照片

Fig. 3 Hand specimens and photomicrographs of the Tanchong and Chenchong stocks

(a)—谭冲岩体手标本照片;(b)—陈冲岩体手标本照片;(c)—谭冲岩体正交偏光显微照片,中细粒花岗岩;

(d)—陈冲岩体正交偏光显微照片,花岗斑岩;Or—正长石;Pl—斜长石;Qtz—石英;Bi—黑云母

(a)—Hand-specimen of the Tanchong granite; (b)—hand-specimen of the Chenchong granite porphyry; (c)—photomicrograph of the Tanchong granite; (d)—photomicrograph of the Chenchong granite porphyry; Or—orthoclase; Pl—plagioclase; Qtz—quartz; Bi—biotite

素进行指数归一化质量歧视校正(Blichert-Toft et al., 1997)。锆石标样 GJ-1 的 $^{176}\text{Hf}/^{177}\text{Hf}$ 标准值为 0.282013 ± 19 (Hu Zhaochu et al., 2012a)。对分析数据的离线处理(包括对样品和空白信号的选择、Lu-Yb-Hf 同位素比值校正)采用软件 ICPMSDataCal (Liu Yongsheng et al., 2010) 完成。

4 测试结果

4.1 锆石 U-Pb 同位素测年

双目镜和显微镜下观察显示,谭冲和陈冲岩体的锆石自形程度高,晶型很好,多呈短柱状或长柱状,无色—浅褐色,透明程度较好。颗粒大小中等,长度 $80 \sim 150\mu\text{m}$ 之间,宽 $40 \sim 80\mu\text{m}$ 。阴极发光图像显示绝大多数锆石均具有清晰的单期生长的同心

环带特征(图 4)。锆石 Th/U 比值范围为 $0.54 \sim 2.72$ 。上述特征共同指示了单一的岩浆锆石成因(Wu Yuanbao et al., 2004)。测试结果见表 1。

对谭冲岩体样品 D003 选取 16 颗锆石进行了 16 个测点的 LA-ICP-MS 分析。全部数据点均分布 U-Pb 谱和线上或其附近(图 5a)。数据点 $^{206}\text{Pb}/^{238}\text{U}$ 年龄相对集中,范围集中在 $131 \sim 140\text{Ma}$,加权平均值为 $133.5 \pm 1.1\text{Ma}$ (MSWD=0.63),代表了谭冲花岗岩的结晶年龄。

对陈冲岩体样品 D011 选取 18 颗锆石进行了 18 个测点的 LA-ICP-MS 分析。全部数据点均分布 U-Pb 谱和线上或其附近(图 5b)。其 $^{206}\text{Pb}/^{238}\text{U}$ 年龄相对集中,范围集中在 $130 \sim 137\text{Ma}$,加权平均值为 $132.9 \pm 1.1\text{Ma}$ (MSWD=2.3),代表了陈冲花岗斑岩的结晶年龄。

4.2 岩石地球化学

谭冲和陈冲岩体样品的主量和微量元素的分析结果列于表 2。两个岩体表现出相似的岩石地球化学特征。

谭冲岩体具较高的 SiO_2 (69.40%~77.82%)、总碱 ($\text{Na}_2\text{O} + \text{K}_2\text{O}$ = 6.40%~8.70%)、 Al_2O_3 (11.72%~15.26%) 含量, $\text{K}_2\text{O}/\text{Na}_2\text{O}$ 比值介于 0.26~3.57, 和较低的 MgO (0.27%~0.99%)、 TiO_2 (0.29%~0.43%)、 FeO^T (1.91%~2.95%) 含量。 $\text{Mg}^{\#}$ 值为 16~42, 碱度率 AR 范围 2.74~3.72, 铝饱和指数 A/CNK 值为 0.97~1.66。样

品在 SiO_2 - K_2O 关系图上总体落在高钾钙碱性系列 (一个样品点落入低钾系列), 在 A/CNK-A/NK 关系图上投点在准铝质—过铝质系列 (图 6)。岩石稀土元素总量介于 137~217 $\mu\text{g/g}$, 轻稀土富集, 重稀土平坦, $(\text{La/Yb})_N$ 为 23.02~28.64, 负 Eu 异常不明显 ($\delta\text{Eu} = 0.80 \sim 0.92$)。大离子亲石元素相对富集, 而亏损 Ba、Nb、Ta、P、Ti 和 Y, 且富集 Pb (图 7)。

陈冲岩体具较高的 SiO_2 (71.21%~75.96%)、总碱 ($\text{Na}_2\text{O} + \text{K}_2\text{O}$ = 7.02%~8.13%)、 Al_2O_3 (12.85%~14.89%) 含量, $\text{K}_2\text{O}/\text{Na}_2\text{O}$ 比值介于

表 1 谭冲和陈冲岩体 LA-ICP-MS 锆石 U-Pb 同位素测定结果

Table 1 LA-ICP-MS zircon isotopic U-Pb data for the Tanchong and Chenchong granites

样品 测点	元素含量($\mu\text{g/g}$)				同位素比值						同位素年龄(Ma)					
	Pb	Th	U	Th/U	$^{207}\text{Pb}/^{206}\text{Pb}$	1σ	$^{207}\text{Pb}/^{235}\text{U}$	1σ	$^{206}\text{Pb}/^{238}\text{U}$	1σ	$^{207}\text{Pb}/^{206}\text{Pb}$	1σ	$^{207}\text{Pb}/^{235}\text{U}$	1σ	$^{206}\text{Pb}/^{238}\text{U}$	1σ
样品 D003: 谭冲花岗岩																
D003@01	210	1481	1502	0.99	0.0494	0.0020	0.1432	0.0066	0.0209	0.0005	169	90	136	6	134	3
D003@02	103	778	366	2.13	0.0515	0.0030	0.1462	0.0078	0.0210	0.0004	265	135	139	7	134	2
D003@03	70	488	233	2.10	0.0537	0.0034	0.1484	0.0082	0.0209	0.0004	367	144	141	7	134	3
D003@04	70	542	264	2.06	0.0486	0.0031	0.1399	0.0080	0.0214	0.0004	132	144	133	7	136	3
D003@05	53	308	210	1.47	0.0504	0.0053	0.1492	0.0135	0.0220	0.0006	213	230	141	12	140	4
D003@06	33	209	295	0.71	0.0490	0.0031	0.1385	0.0086	0.0208	0.0006	146	154	132	8	133	4
D003@07	104	638	954	0.67	0.0527	0.0022	0.1535	0.0070	0.0209	0.0004	322	93	145	6	133	3
D003@08	563	5030	1236	4.07	0.0491	0.0016	0.1421	0.0046	0.0209	0.0002	154	76	135	4	133	1
D003@09	299	2172	1916	1.13	0.0511	0.0019	0.1469	0.0055	0.0207	0.0003	256	82	139	5	132	2
D003@10	221	1697	1259	1.35	0.0463	0.0017	0.1344	0.0052	0.0209	0.0003	13	85	128	5	133	2
D003@11	132	994	508	1.96	0.0500	0.0019	0.1450	0.0057	0.0209	0.0003	195	89	138	5	134	2
D003@12	53	388	358	1.08	0.0495	0.0027	0.1475	0.0083	0.0214	0.0004	172	128	140	7	137	2
D003@13	147	1108	646	1.72	0.0567	0.0023	0.1633	0.0064	0.0211	0.0005	479	68	154	6	134	3
D003@14	990	6552	2408	2.72	0.0461	0.0036	0.1307	0.0100	0.0206	0.0004	606	172	125	9	131	2
D003@15	160	1151	618	1.86	0.0550	0.0029	0.1594	0.0091	0.0209	0.0004	411	121	150	8	133	3
D003@16	144	805	1499	0.54	0.0487	0.0025	0.1394	0.0068	0.0207	0.0003	135	116	132	6	132	2
样品 D011: 陈冲花岗斑岩																
D011@01	56	421	212	1.99	0.0492	0.0044	0.1435	0.0128	0.0212	0.0005	167	187	136	11	135	3
D011@02	15	107	75	1.42	0.0517	0.0056	0.1428	0.0130	0.0213	0.0006	272	51	136	12	136	4
D011@03	11	73	51	1.45	0.0498	0.0091	0.1447	0.0231	0.0215	0.0009	183	381	137	21	137	6
D011@04	74	558	336	1.66	0.0474	0.0024	0.1394	0.0072	0.0214	0.0003	78	109	133	6	136	2
D011@05	42	310	250	1.24	0.0509	0.0033	0.1430	0.0082	0.0213	0.0004	239	153	136	7	136	3
D011@06	125	966	412	2.34	0.0494	0.0026	0.1439	0.0071	0.0212	0.0003	169	124	137	6	136	2
D011@07	189	1547	1243	1.24	0.0493	0.0027	0.1399	0.0072	0.0206	0.0003	167	125	133	6	132	2
D011@08	139	1086	654	1.66	0.0538	0.0029	0.1511	0.0077	0.0204	0.0003	365	124	143	7	130	2
D011@09	130	1084	461	2.35	0.0507	0.0022	0.1412	0.0058	0.0204	0.0003	228	102	134	5	130	2
D011@10	113	857	419	2.05	0.0480	0.0023	0.1343	0.0062	0.0205	0.0003	98	111	128	6	131	2
D011@11	123	919	1019	0.90	0.0483	0.0016	0.1358	0.0042	0.0204	0.0003	122	78	129	4	130	2
D011@12	189	1377	1231	1.12	0.0500	0.0019	0.1421	0.0054	0.0205	0.0003	195	89	135	5	131	2
D011@13	36	259	150	1.72	0.0515	0.0041	0.1451	0.0100	0.0213	0.0004	265	181	138	9	136	3
D011@14	120	881	358	2.46	0.0498	0.0025	0.1454	0.0072	0.0212	0.0003	183	119	138	6	136	2
D011@15	20	158	94	1.69	0.0495	0.0059	0.1319	0.0134	0.0212	0.0006	172	259	126	12	135	4
D011@16	154	1100	848	1.30	0.0506	0.0020	0.1485	0.0061	0.0213	0.0003	220	99	141	5	136	2
D011@17	64	344	316	1.09	0.0574	0.0068	0.1635	0.0191	0.0206	0.0004	508	269	154	17	132	3
D011@18	257	1679	1216	1.38	0.0666	0.0048	0.1920	0.0133	0.0209	0.0004	825	154	178	11	133	2

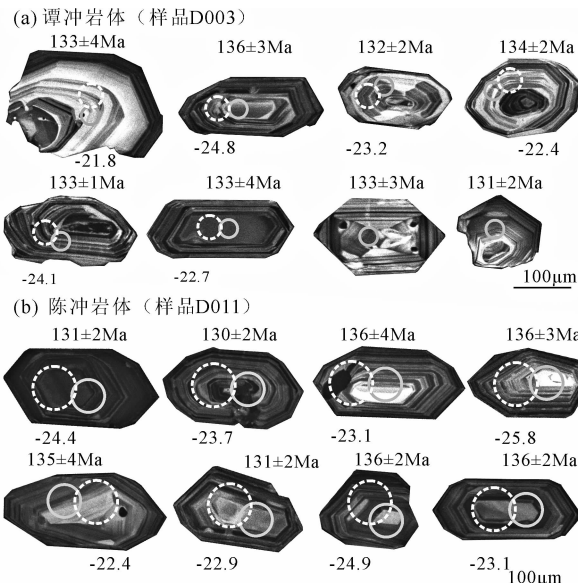


图 4 谭冲和陈冲岩体代表性锆石阴极发光(CL)图像、激光点 U-Pb 年龄及 $\epsilon_{\text{Hf}}(t)$ 值

Fig. 4 Cathodoluminescence images, LA-ICP-MS U-Pb (small circles) and in-situ Hf determination spots (big circles in dotted lines) with ages and $\epsilon_{\text{Hf}}(t)$ results of representative zircons for the Tanchong and Chenchong granites

1.31~1.44, 和较低的 MgO (0.23%~0.66%)、
TiO₂ (0.20%~0.42%)、FeO^T (1.43%~2.63%) 含

量。Mg[#] 值为 22~35, 碱度率 AR 范围 2.71~3.70, 铝饱和指数 A/CNK 值为 1.25~1.51。样品在 SiO₂-K₂O 关系图上均落在高钾钙碱性系列, 在 A/CNK-A/NK 关系图上投点在强过铝质系列。岩石稀土元素总量介于 188~193 μg/g, 轻稀土富集, 重稀土平坦, (La/Yb)_N 为 22.98~28.48, 负 Eu 异常不明显(或弱负 Eu 异常), $\delta\text{Eu}=0.56\sim0.86$ 。大离子亲石元素相对富集, 而亏损 Ba、Nb、Ta、P、Ti 和 Y, 且富集 Pb。

4.3 全岩 Sr-Nd 同位素

谭冲和陈冲岩体的全岩 Sr-Nd 同位素分析结果列于表 3。两个岩体表现出非常相似的 Sr-Nd 同位素组成特征。参照成岩年龄 ($t=133\text{ Ma}$) 计算, 获得其全岩初始 Sr 比值 ($^{87}\text{Sr}/^{86}\text{Sr}$)_i = 0.707220~0.707557; Nd 同位素初始比值 ($^{143}\text{Nd}/^{144}\text{Nd}$)_i = 0.511538~0.511560, $\epsilon_{\text{Nd}}(t) = -17.7\sim-18.1$ 。利用两阶段模式 (Liew et al., 1988) 计算出 Nd 同位素两阶段模式年龄 $T_{2\text{DM}} = 2.36\sim2.40\text{ Ga}$, 均值为 2.38Ga。

4.4 锆石 Lu-Hf 同位素

在 LA-ICP-MS 锆石 U-Pb 测年基础上, 对两个岩体样品 D003 和 D011 进行了锆石微区 Hf 同位

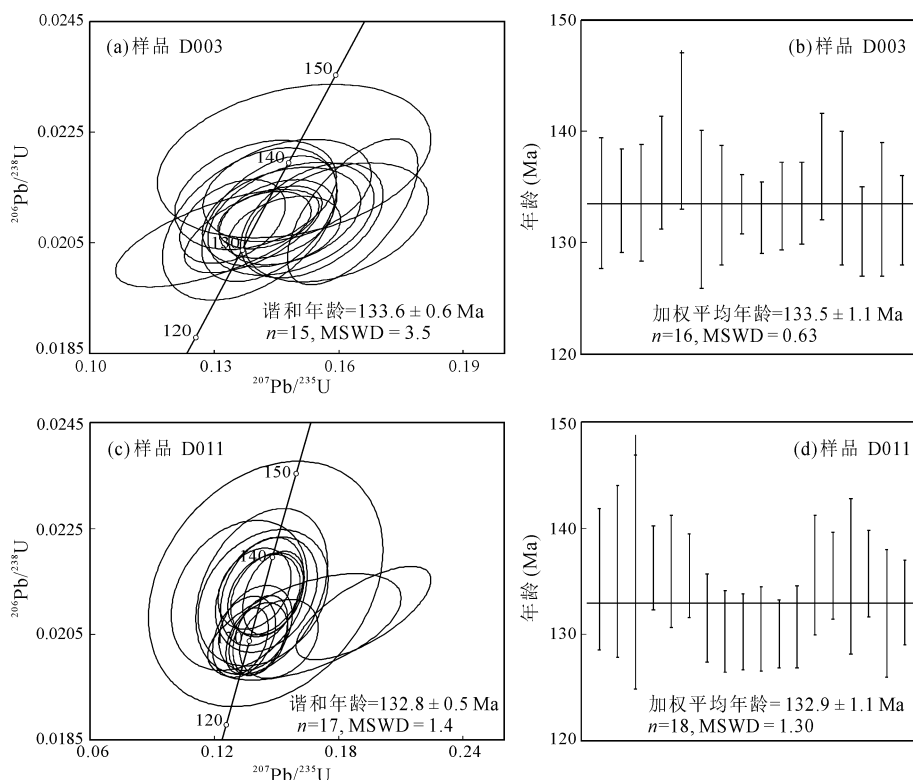


图 5 谭冲(a, b)和陈冲岩体(c, d)锆石 U-Pb 年龄

Fig. 5 U-Pb concordia diagrams and weighted mean ages for the Tanchong (a, b) and Chenchong (c, d) granites

表 2 谭冲和陈冲岩体主量元素(%)和微量元素、

稀土元素($\mu\text{g/g}$)分析结果Table 2 Major elements (%), trace elements ($\mu\text{g/g}$) and rare earth elements ($\mu\text{g/g}$) of the Tanchong and Chenchong granites

岩体	谭冲岩体				陈冲岩体		
	D015	D013-1	D003	D016	D0011-3	D0012-1	D0012-2
SiO ₂	77.82	70.66	69.40	70.54	71.21	71.45	75.96
Al ₂ O ₃	11.72	14.88	14.13	15.26	14.42	14.89	12.85
Fe ₂ O ₃	1.09	1.83	1.87	1.98	1.72	1.69	0.52
FeO	0.93	1.30	1.14	1.07	0.99	1.11	0.96
CaO	0.26	0.22	1.81	0.28	0.44	0.35	0.17
MgO	0.27	0.28	0.99	0.52	0.66	0.34	0.23
K ₂ O	1.33	5.20	4.48	5.64	4.61	4.14	4.36
Na ₂ O	5.07	3.50	3.91	1.58	3.52	2.88	3.12
TiO ₂	0.29	0.38	0.36	0.43	0.38	0.42	0.20
P ₂ O ₅	0.13	0.07	0.13	0.11	0.15	0.16	0.04
MnO	0.04	0.06	0.07	0.05	0.05	0.04	0.05
L. O. I.	0.70	1.10	1.16	2.08	1.38	2.05	1.17
Total	99.64	99.48	99.44	99.53	99.53	99.52	99.64
A/NK	1.20	1.31	1.25	1.75	1.34	1.62	1.30
A/CNK	1.14	1.26	0.97	1.66	1.25	1.51	1.26
La	36.2	49.1	43.4	57.5	50.3	51.4	54.4
Ce	63.0	83.1	74.5	99.1	87.8	88.8	89.8
Pr	6.63	9.11	7.84	10.5	9.15	9.28	8.44
Nd	19.9	28.0	24.1	32.4	28.4	28.4	23.1
Sm	3.37	4.95	4.22	5.59	4.98	4.79	3.51
Eu	0.73	1.15	1.04	1.22	1.16	1.07	0.55
Gd	2.29	3.29	2.82	3.64	3.40	3.15	2.59
Tb	0.36	0.52	0.44	0.54	0.52	0.47	0.38
Dy	1.86	2.68	2.22	2.67	2.71	2.42	1.96
Ho	0.36	0.51	0.42	0.49	0.52	0.47	0.38
Er	1.04	1.43	1.20	1.37	1.43	1.32	1.12
Tm	0.16	0.23	0.19	0.21	0.22	0.21	0.19
Yb	1.11	1.53	1.34	1.44	1.57	1.44	1.37
Lu	0.15	0.21	0.19	0.19	0.22	0.20	0.19
Y	8.78	13.0	10.8	12.0	13.1	11.1	9.68
Li	8.00	4.22	12.4	11.1	11.5	21.4	9.91
Cr	19.8	27.6	35.3	38.9	27.6	30.3	8.35
Co	3.43	5.54	5.69	5.66	5.54	5.54	1.72
Ni	9.91	12.0	14.0	14.8	15.6	15.3	5.31
Ga	16.1	32.7	39.5	27.9	31.1	30.4	19.0
Nb	10.1	13.7	13.3	14.8	13.1	13.1	14.2
Mo	1.84	1.02	0.92	1.25	0.54	1.31	0.77
Ta	1.10	1.56	1.47	1.56	1.41	1.38	1.31
Th	11.8	14.2	15.4	16.2	16.3	16.1	25.7
U	2.66	2.96	5.46	2.69	3.98	3.14	4.05
Cl	69.4	86.0	109	126	104	92.2	99.8
Ba	249	1130	1640	796	1040	946	376
Hf	3.02	4.56	4.22	4.80	4.34	4.37	4.50
Pb	32.8	21.0	39.9	23.3	29.6	29.7	39.2
Rb	46.1	157	136	217	129	125	128
Sr	149	240	474	93.0	211	180	89.2
Zr	79.2	121	115	140	123	125	106
Cs	1.84	3.45	2.23	6.85	2.55	4.30	1.86
As	0.93	0.91	0.85	1.02	0.92	1.58	1.34
Sb	0.26	0.19	0.15	0.34	0.30	0.26	0.22

续表 2

岩体	谭冲岩体				陈冲岩体		
	D015	D013-1	D003	D016	D0011-3	D0012-1	D0012-2
Bi	0.91	0.12	0.27	0.09	0.28	0.20	0.16
Be	1.28	2.77	3.13	3.18	2.69	2.62	2.74
V	24.4	30.7	32.7	38.4	34.9	40.6	10.0
Sc	3.49	5.03	5.09	4.50	6.45	5.73	2.26
Cu	35.2	9.17	9.61	7.44	9.71	16.6	5.40
Zn	39.0	34.2	41.7	29.8	40.9	61.2	30.8
Au	0.54	0.53	0.50	0.62	0.57	0.41	3.62
Ag	0.36	0.08	0.12	0.05	0.05	0.14	0.06
Σ REE	137	186	164	217	192	193	188
(La/Yb) _N	23.39	23.02	23.23	28.64	22.98	25.60	28.48
δ Eu	0.80	0.87	0.92	0.83	0.86	0.84	0.56
δ Ce	1.00	0.96	0.99	0.99	1.00	1.00	1.03

素测定, 分析结果见表 4 和图 8。几乎全部锆石的 $^{176}\text{Lu}/^{177}\text{Hf}$ 比值小于 0.002, 说明锆石在形成后具有很少的放射成因 Hf 的积累, 所测定的 $^{176}\text{Hf}/^{177}\text{Hf}$ 比值基本代表了其形成时体系的 Hf 同位素组成。

谭冲岩体(样品 D003)测得锆石 $^{176}\text{Hf}/^{177}\text{Hf}$ 和 $^{176}\text{Lu}/^{177}\text{Hf}$ 值分别为 0.281990~0.282059 和 0.000893~0.001726。根据锆石 U-Pb 年龄计算的 $\epsilon_{\text{Hf}}(t)$ 值集中于 -21.8~-24.8, 平均值为 -23.2, 两阶段 Hf 模式年龄介于 2.26~2.42Ga。

陈冲岩体(样品 D011)分析了 12 个激光点, 测得 $^{176}\text{Hf}/^{177}\text{Hf}$ 和 $^{176}\text{Lu}/^{177}\text{Hf}$ 值分别为 0.281961~0.282084 和 0.001230~0.002269。根据锆石 U-Pb 年龄计算的 $\epsilon_{\text{Hf}}(t)$ 值集中于 -21.4~-25.8, 平均值为 -23.6, 两阶段模式年龄介于 2.24~2.48Ga。

5 讨论

5.1 岩石成因类型

S型和 I型花岗岩成因类型由 Chappell et al. (1974; 1992) 提出, 被广泛运用至今。S型花岗岩源岩为地壳沉积物, 多形成于大陆碰撞造山环境; I型花岗岩源岩为火成岩, 多形成于科迪勒拉型造山环境。强过铝质特征(A/CNK 值>1.1)是 S型花岗岩重要地球化学判断指标之一, 但这一指标可能并不适用于高分异花岗岩(Chappell, 1999; Wu Fuyuan et al., 2007; Li Xianhua et al., 2007)。矿物组成对花岗岩成因类型具有更重要的指示性。堇青石和角闪石分别是判别 S型和 I型花岗岩的重要矿物学标志(Wu Fuyuan et al., 2017)。

谭冲和陈冲岩体的主要岩性分别为中细粒二长花岗岩和花岗斑岩。两个岩体地球化学特征非常相似, 均具有高硅、富碱特征, 属于高钾钙碱性系列, 总

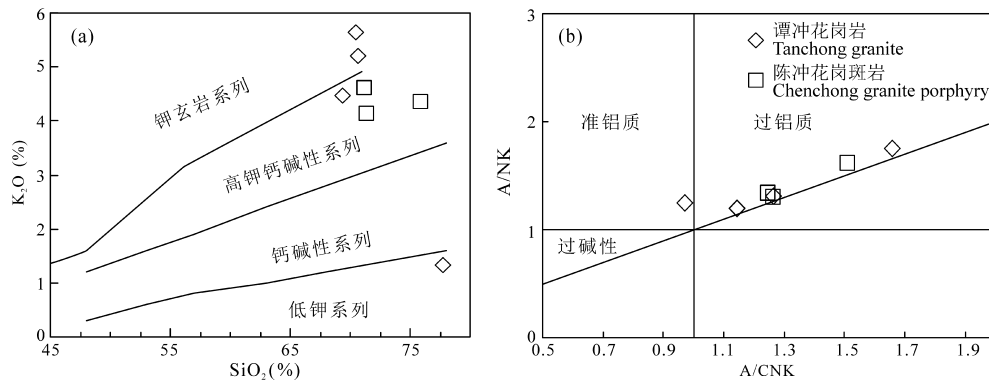


图 6 谭冲和陈冲岩体主量元素图解

Fig. 6 Major element diagrams for the Tanchong and Chenchong granites

表 3 谭冲和陈冲岩体全岩 Sr-Nd 同位素分析结果

Table 3 Rb-Sr and Sm-Nd isotopic data of the Tanchong and Chenchong granites

样品号	岩体/岩性	年龄 (Ma)	Rb (μ g/g)	Sr (μ g/g)	$^{87}Rb/^{86}Sr$	$^{87}Sr/^{86}Sr$	I_{Sr}	Sm (μ g/g)	Nd (μ g/g)	$^{147}Sm/^{144}Nd$	$^{143}Nd/^{144}Nd$	$(^{143}Nd/^{144}Nd)_i$	$\epsilon_{Nd}(t)$	T_{2DM} (Ga)
D003	谭冲花岗岩	133	133.6	452.60	0.8514	0.70887	0.707261	3.638	22.960	0.0959	0.511621	0.511538	-18.1	2.40
D015	谭冲花岗岩	133	50.58	163.60	0.8913	0.70918	0.707495	3.945	26.690	0.0894	0.511638	0.511560	-17.7	2.36
D0011-3	陈冲花岗斑岩	133	136.0	226.10	1.735	0.71050	0.707220	4.277	26.910	0.0962	0.511629	0.511545	-18.0	2.39
D0012-1	陈冲花岗斑岩	133	128.9	210.90	1.763	0.71089	0.707557	3.995	26.670	0.0906	0.511631	0.511552	-17.8	2.37

注: 计算过程所用参数: $(^{147}Sm/^{143}Nd)_{CHUR} = 0.1967$; $(^{143}Nd/^{144}Nd)_{CHUR} = 0.512638$; $(^{147}Sm/^{143}Nd)_{DM} = 0.2127$; $(^{143}Nd/^{144}Nd)_{DM} = 0.51315$ 。

表 4 谭冲和陈冲岩体的锆石 Lu-Hf 同位素 LA-MC-ICP-MS 原位分析结果

Table 4 LA-MC-ICP-MS zircon Lu-Hf isotopic data of the Tanchong and Chenchong granites

激光点号	年龄(Ma)	$^{176}Lu/^{177}Hf$	$^{176}Yb/^{177}Hf$	$^{176}Hf/^{177}Hf$	1σ	$\epsilon_{Hf}(0)$	1σ	$\epsilon_{Hf}(t)$	1σ	t_{2DM}	$f_{Lu/Hf}$
D003: 谭冲花岗岩											
D003@02	134	0.001560	0.074513	0.282059	0.000014	-25.2	0.7	-22.4	0.7	2.29	-0.95
D003@04	136	0.001504	0.078842	0.281990	0.000014	-27.6	0.7	-24.8	0.7	2.42	-0.95
D003@06	133	0.000893	0.038057	0.282074	0.000011	-24.7	0.7	-21.8	0.7	2.26	-0.97
D003@08	133	0.001726	0.085799	0.282013	0.000014	-26.8	0.7	-24.1	0.7	2.38	-0.95
D003@09	132	0.000936	0.033754	0.282094	0.000013	-24.0	0.7	-23.2	0.7	2.34	-0.97
D003@10	133	0.001678	0.077760	0.282053	0.000014	-25.4	0.7	-22.7	0.7	2.30	-0.95
D011: 陈冲花岗斑岩											
D011@02	136	0.001230	0.058850	0.282038	0.000015	-26.0	0.7	-23.1	0.8	2.33	-0.96
D011@03	137	0.001381	0.069359	0.282084	0.000013	-24.3	0.7	-21.4	0.7	2.24	-0.96
D011@04	136	0.001919	0.100961	0.282047	0.000014	-25.6	0.7	-22.8	0.7	2.32	-0.94
D011@05	136	0.000771	0.040307	0.281961	0.000013	-28.7	0.7	-25.8	0.7	2.48	-0.98
D011@06	136	0.001955	0.103180	0.281971	0.000015	-28.3	0.7	-25.5	0.8	2.46	-0.94
D011@08	130	0.001451	0.067354	0.282025	0.000013	-26.4	0.7	-23.7	0.7	2.36	-0.96
D011@10	131	0.001796	0.090349	0.282049	0.000015	-25.6	0.7	-22.9	0.7	2.31	-0.95
D011@11	130	0.001839	0.079137	0.282036	0.000014	-26.0	0.7	-23.3	0.7	2.34	-0.94
D011@12	131	0.002009	0.092016	0.282007	0.000012	-27.0	0.7	-24.4	0.7	2.39	-0.94
D011@14	136	0.002269	0.114828	0.281990	0.000014	-27.7	0.7	-24.9	0.7	2.43	-0.93
D011@15	135	0.001381	0.063344	0.282057	0.000013	-25.3	0.7	-22.4	0.7	2.29	-0.96
D011@16	136	0.001814	0.088321	0.282041	0.000012	-25.9	0.7	-23.1	0.7	2.33	-0.95

体表现为强过铝质特征 (A/CNK 值主要介于 1.14 ~ 1.66, 有一个样品除外); 据 CIPW 标准矿物计算, 刚玉含量达 1.84% ~ 6.48%。这些化学特征暗示岩石与 S 型花岗岩地球化学的亲缘性。但是, 对 S 型花岗岩最重要的判断标志是其原生过铝质特征

矿物(如石榴子石、电气石、堇青石、白云母等)。镜下薄片观察表明, 谭冲和陈冲岩体中未见强过铝质矿物, 但发育角闪石(含量约 5%), 支持其可能为 I 型花岗岩。岩石 P_2O_5 含量不高 (0.04% ~ 0.16%), 亦与典型 S 型花岗岩 ($>0.12\%$) 存在差

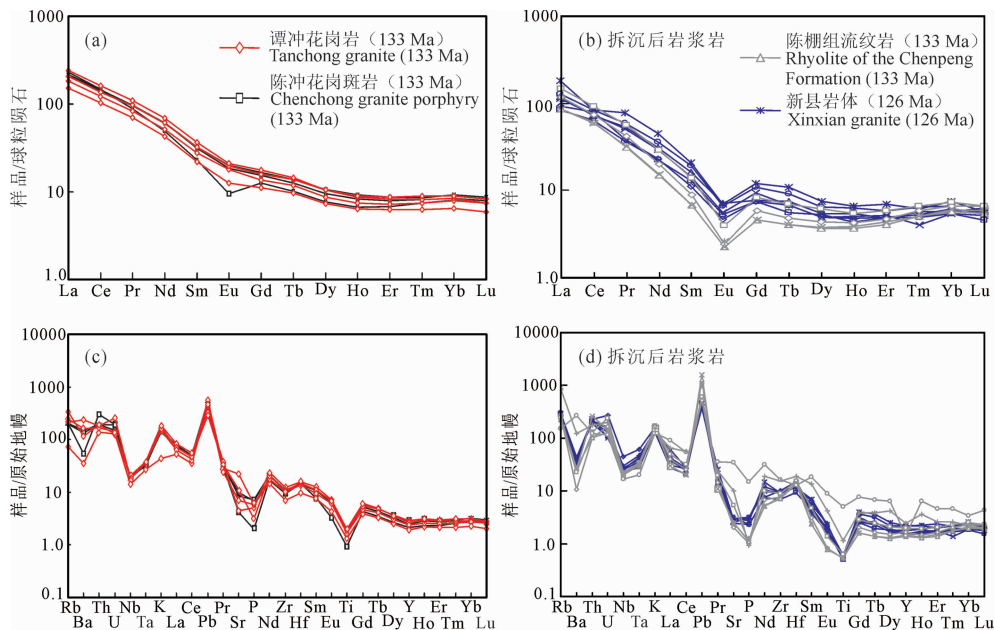


图 7 谭冲和陈冲岩体稀土元素配分图(a)和微量元素原始地幔标准化蛛网图(c),
及其与陈棚组流纹岩和新县花岗岩对比(b, d)

Fig. 7 Chondrite-normalized REE pattern for the Tanchong and Chenchong granites (a), comparing with the Chenpeng volcanics and the Xinxiang granite (b), and primitive mantle-normalized trace elements diagram for the Tanchong and Chenchong granites (c), comparing with the Chenpeng volcanics and the Xinxiang granite (d)

陈棚组火山岩数据引自 Zhu Jiang et al. (2018a); 新县岩体数据引自 Chen Wei et al. (2013a); 标准化数据 Sun et al., 1989
The Chenpeng volcanics and the Xinxiang granite data according to Zhu Jiang et al. (2018a) and Chen Wei et al. (2013a),
respectively; normalized values are from Sun et al., 1989

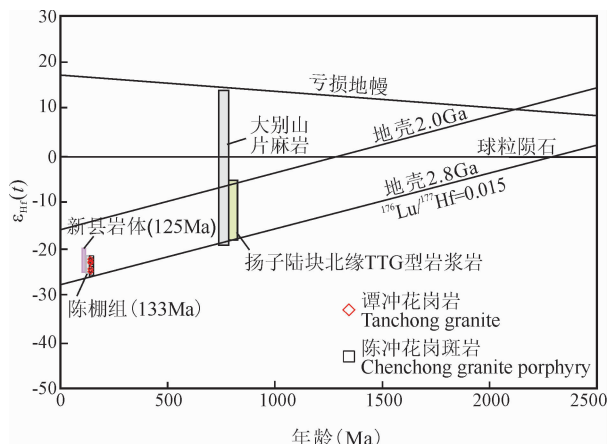


图 8 谭冲和陈冲岩体锆石 $\epsilon_{\text{Hf}}(t)$ -t 图解

Fig. 8 Zircon $\epsilon_{\text{Hf}}(t)$ vs. age diagram for the Tanchong and Chenchong granites

陈棚组火山岩数据引自文献 Zhu Jiang et al. (2018a); 新县岩体数据引自 Chen Wei et al. (2013a)

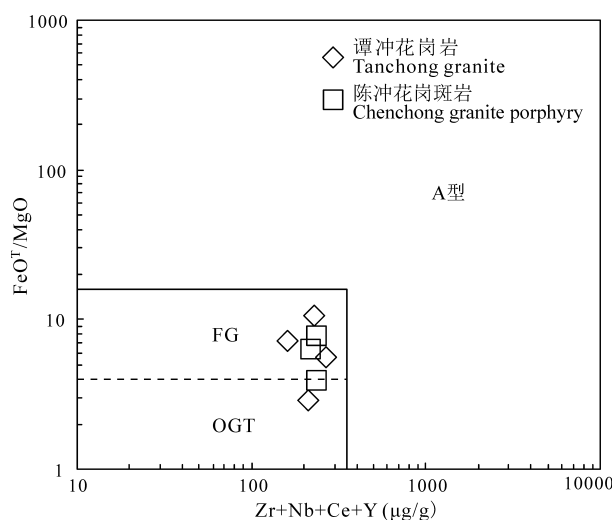
The Chenpeng volcanics and the Xinxiang granite data according to Zhu Jiang et al. (2018a) and Chen Wei et al. (2013a), respectively

异。两个岩体样品在 FeO^T/MgO vs. $(\text{Zr} + \text{Nb} + \text{Ce} + \text{Y})$ 关系图上样品均落入高分异花岗岩区域 (图 9);微量元素特征亦反映岩石经过了较高程度

结晶分异。另外,岩石的 $\text{Zr} + \text{Nb} + \text{Ce} + \text{Y}$ 含量介于 $161 \sim 266 \mu\text{g/g}$ 之间,REE 含量不高,负 Eu 异常不明显,这些特征排除了 A 型花岗岩的可能。结合矿物组成、地球化学和 Sr-Nd-Hf 同位素特征认为,谭冲和陈冲岩体表现出分异的花岗岩特征,成因类型更可能归属于分异的 I 型花岗岩。

5.2 岩浆源区

前人研究多认为,大别山早白垩世花岗岩是扬子地块北缘中下地壳部分熔融的产物(Huang Jie et al., 2006; Zhao Zifu et al., 2007, 2009; Chen Wei et al., 2013a)。Chen Wei et al. (2013a)对大别白垩纪花岗岩、大别杂岩以及扬子北缘新元古代 TTG 型岩浆岩 Sr-Nd-Hf 同位素对比研究认为:白垩纪花岗岩与大别杂岩在 Sr-Nd 同位素组成上相似,但二者 Hf 同位素组成具明显差异,其源岩可能是扬子陆壳北缘新元古代 TTG 型岩浆岩。但是该文所对比的扬子陆壳北缘新元古代 TTG 型岩浆岩出露于鄂西黄陵地区,位置远离大别造山带,仅可能一定程度反映了区域扬子地块基底同位素性质。笔者近期对西大别地区新元古代片麻质花岗岩 Hf 同位素研究表明,其锆石 $\epsilon_{\text{Hf}}(t)$ 值介于 $-19.2 \sim +5.6$ 之间

图 9 谭冲和陈冲岩体 FeO^T/MgO -($\text{Zr}+\text{Nb}+\text{Ce}+\text{Y}$) 图解Fig. 9 FeO^T/MgO versus ($\text{Zr}+\text{Nb}+\text{Ce}+\text{Y}$) diagram

for the Tanchong and Chenchong granites

FG—分异的花岗岩, OGT—未分异的 M-, I- 和 S-型花岗岩

FG—Fractionated felsic granite;

OGT—unfractionated M-, I- and S-type granite

($T_{\text{DM2}}=1.26 \sim 2.58 \text{ Ga}$, Zhu Jiang et al., 2018a),更明确地反映了西大别地区扬子陆壳的性质。由此揭示,白垩纪花岗岩与大别基底岩石在 Sr-Nd-Hf 同位素组成上均具相似性,暗示其与扬子陆壳在源区上的亲缘性。

谭冲和陈冲岩体地球化学特征具有较高的 SiO_2 、总碱含量, $\text{K}_2\text{O}/\text{Na}_2\text{O}$ 比值大于 1, 暗示其与成熟大陆地壳的亲缘性。岩石具较低的 Sr 同位素初始比值($^{87}\text{Sr}/^{86}\text{Sr}$)_i=0.707220~0.707557), 非常负的 ϵ_{Nd} 值(-17.7~-18.1), 二阶段 Nd 同位素模式年龄 $T_{\text{DM2}}=2.36 \sim 2.40 \text{ Ga}$, 在 Sr-Nd 图解上样品点与大别山白垩纪花岗岩范围一致, 落入扬子下地壳附近(图 10), 暗示两个岩体是扬子板块北缘地壳部分熔融的产物。锆石 Hf 同位素特征揭示, 两个岩体锆石的 $\epsilon_{\text{Hf}}(t)$ 值均集中于 -25.8~-21.4 之间, T_{DM2} 值范围为 2.24~2.48Ga, 进一步表明两个岩体源于古老的地壳物质的部分熔融。相似的元素地球化学和 Sr-Nd-Hf 同位素组成暗示, 两个岩体源区物质和成岩条件相似。Sr-Nd-Hf 同位素组成变化范围较小, 指示了岩浆源区相对简单均一, 无明显幔源物质加入以及岩浆混合等复杂成岩作用参与。综上, 谭冲和陈冲岩体可能是扬子北缘古老地壳物质部分熔融的产物。

实验岩石学研究表明, 不同压力条件下部分熔融产生的熔体和残留体存在较大差异, 借此可判断

母岩浆形成的压力和深度(Nair et al., 2008)。谭冲和陈冲岩体具富集 LREE、亏损 HREE, 极弱负 Eu 异常($\delta\text{Eu}=0.84 \sim 0.92$, 仅一个样品除外), 且亏损 Y, 表明岩浆源区残留相含石榴子石。极弱负 Eu 异常暗示岩浆源区很少斜长石残留。上述特征暗示, 岩浆可能起源于残留相富含石榴子石的部分熔融熔体。根据部分熔融实验, 石榴子石稳定出现的压力至少大于 0.8~1.0 GPa, 通常大于 1.5 GPa, 母岩浆形成深度至少大于 40km (Xiong et al., 2005; Nair and Chacko, 2008)。另外, 谭冲岩体中角闪石的发育, 也是区域内形成于深度大于 50km 加厚下地壳部分熔融产物的重要标志(Chen Wei et al., 2013a)。因此, 我们认为谭冲和陈冲岩体地球化学性质上与姚冲(Chen Wei et al., 2015)、千鹅冲岩体(Gao Yang et al., 2014)相似, 其母岩浆形成压力条件较高, 可能形成于加厚下地壳环境。

5.3 动力学背景和对拆沉时限约束

大别造山带形成于三叠纪扬子与华北板块之间的碰撞对接(Ames et al., 1993; Hacker et al., 1998; Ratschbacher et al., 2003)。区域超高压变质岩研究显示造山带内扬子陆壳曾向北深俯冲到 100~200km 的深度, 并且部分陆壳发生折返(Wang Chunyong et al., 2000)。地球物理资料表明, 该造山带现今地壳的平均厚度约为 35km, 且缺少基性下地壳, 表明该造山带曾经发生了加厚下地壳的拆沉(Gao Shan et al., 1999), 由此诱发了强烈而广泛的白垩纪岩浆活动。对于大别造山带白垩纪拆沉作用时限的限定, 更多地依靠区域岩浆岩年代学和地球化学研究。大别地区早于 132Ma 的花岗岩多具有高 Sr/Y 比值以及低 Y 含量的特征, 可能形成于深度大于 50km 加厚下地壳的部分熔融; 晚于 130Ma 的花岗岩不再具有上述地球化学特征, 可能形成于地壳物质在深度小于 35km 下地壳物质的部分熔融(He Yongsheng et al., 2007; Xu Haijin et al., 2007)。由此认为, 大别造山带加厚下地壳拆沉作用发生在 132Ma 左右(Jahn et al., 1999; Zhao Zifu et al., 2005, 2007, 2008; Xu Haijin et al., 2007, 2013; Xu Yixian et al., 2016; Huang Fang et al., 2007; Zhang Chao et al., 2008)。Chen Wei et al.(2013a)指出, 侵位时限、岩体形变和是否含角闪石是区分拆沉前、后两期岩浆岩的重要标志。

目前对大别山白垩纪加厚下地壳拆沉时限的认识主要基于东大别岩浆岩研究, 对西大别地区岩浆

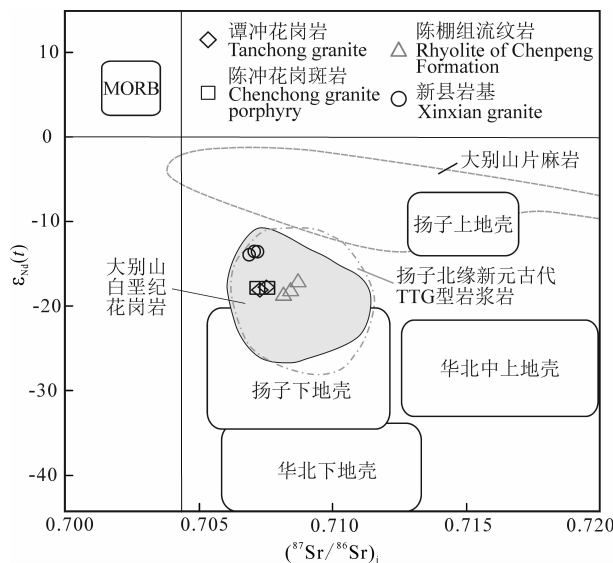


图 10 谭冲和陈冲岩体 Sr-Nd 同位素组成

(底图据 John et al., 1999; Zhao Zifu et al., 2009;
Chen Wei et al., 2013 修改)

Fig. 10 $\epsilon_{\text{Nd}}(t)$ vs. $^{87}\text{Sr}/^{86}\text{Sr}$ diagram for the
Tanchong and Chenchong granites

扬子北缘新元古代 TTG 型岩浆岩数据引自 Zhang Shaobing et al., 2009, 反映了扬子北缘古老下地壳性质; 大别片麻岩数据引自 Ma Changqian et al., 2000; 中生代花岗岩范围引自 Zhao Zifu et al., 2009; 陈棚组火山岩数据引自文献 Zhu Jiang et al., 2018a; 新县岩体数据引自 Chen Wei et al., 2013a

The data for Neoproterozoic TTG-like rocks are from Zhang Shaobing et al., 2009, reflecting the features of the ancient lower crust within the northern Yangtze Block; the data for the Dabie gneiss are from Ma Changqian et al., 2000; the data for Cretaceous granitoids from Dabie are from Zhao Zifu et al., 2009 and references therein; the data for the Chenpeng volcanics and the Xinxian granite are from Zhu Jiang et al., 2018a and Chen Wei et al., 2013a, respectively

岩研究相对薄弱(Chen Wei et al., 2013, 2015, 2016; Gao Xinyu et al., 2013)。西大别地区内 3 个主要岩基(新县岩基 126 ± 2 Ma、灵山岩基 $130 \sim 125$ Ma、夏店岩基 130 ± 2 Ma)从侵位时限和化学特征上看,均形成于拆沉后伸展、非加厚下地壳环境(Chen Wei et al., 2013, 2015, 2016; Gao Xinyu et al., 2013)。区域加厚下地壳拆沉、挤压—伸展转化时限仍存在争议。Gao Xinyu et al. (2013)将商城岩体侵位时限 137 ± 2 Ma 视作构造体制转换的最小时限; Gao Yang et al. (2014)认为在 130 Ma 左右千鹅冲钼矿区范围内加厚下地壳可能局部尚未拆沉; Chen Wei et al. (2015)基于姚冲岩体侵位时限和岩石成因认为,至少在 133 Ma 尚未发生加厚下地壳的大规模拆沉。本文将谭冲、陈冲岩体与区域内

陈棚组流纹岩(侵位时限为约 133 Ma, Du Jianguo et al., 1999; Yang Meizhen et al., 2012; Zhu Jiang et al., 2018a)对比表明:①三者侵位时间接近,获得锆石 U-Pb 年龄均为 133 Ma 左右;②三者具有相似的 Sr-Nd-Hf 同位素组成,均属于 I 型花岗岩,暗示其起源于扬子地壳物质重熔;③稀土和微量元素特征上,谭冲、陈冲岩体具极弱负 Eu 异常和 Y 亏损,可能起源于深度大于 50 km 加厚下地壳;陈棚组火山岩具明显负 Eu 异常且无 Y 亏损(与前者具明显差异),可能起源于深度小于 35 km 的非加厚下地壳(Zhu Jiang et al., 2018a)。进一步结合区内姚冲岩体(拆沉前, Chen Wei et al., 2015)和新县岩体(拆沉后, Chen Wei et al., 2013a)特征认为,西大别造山带加厚下地壳拆沉和构造体制转换发生在 133 Ma 左右,与东大别地区时限基本一致。

综上,西大别地区和东大别地区在白垩纪构造演化具有一致性和整体性,经历了加厚下地壳拆沉,进而导致岩石圈强烈减薄和软流圈上涌。随着造山带山根垮塌,区域近南北向挤压应力被完全释放,进而转入强烈拉张伸展的应力环境(Chen Ling et al., 2009; Li Hailong et al., 2017)。谭冲和陈冲岩体可能形成于加厚下地壳环境,约束了区域挤压—伸展构造体制转换时限。

6 结论

(1) 西大别地区谭冲和陈冲岩体的锆石 U-Pb 年龄分别为 133.1 ± 1.5 Ma 和 133.1 ± 0.8 Ma, 形成于早白垩世。

(2) 谭冲岩体主要造岩矿物为斜长石、钾长石、石英、角闪石和黑云母,陈冲岩体主要造岩矿物为斜长石、钾长石、石英和黑云母。两岩体具有相似元素地球化学特征和 Sr-Nd-Hf 同位素组成,暗示其源区物质组成和成岩条件相似。岩石具高硅、富碱特征, $\text{MgO}/\text{FeO}^{\text{T}}$ 含量较低, 属高钾钙碱性系列, 可能为分异的 I 型花岗岩。岩浆起源于扬子北缘古老地壳物质部分熔融, 母岩浆形成深度和压力较大, 可能形成于加厚下地壳环境。

(3) 结合区域岩浆岩地球化学特征认为, 西大别造山带加厚下地壳拆沉作用发生时限为 133 Ma 左右,与东大别地区时限基本一致。

致谢:野外工作中得到了武汉地质调查中心邓新、徐大良、刘浩的帮助; 撰稿过程中与王磊和贾小辉进行了有益讨论。审稿专家对论文修改提出了宝贵建议,在此致以衷心感谢。

References

- Ames L, Tilton G R, Zhou G Z. 1993. Timing of collision of the Sino-Korean and Yangtze craton: U-Pb zircon dating of coesite-bearing eclogites. *Geology*, 21(4): 339~342.
- Blichert-Toft J, Chauvel C, Albarède F. 1997. Separation of Hf and Lu for high-precision isotope analysis of rock samples by magnetic sector-multiple collector ICP-MS. *Contributions to Mineralogy and Petrology*, 127(3): 248~260.
- Cao Zhengqi, Cai Yitao, Zeng Zuoxun, Hu Zhengxiang, Chen Jing, Jiang Xingfu, Sun Zhengquan, Wu Bo, Liu Chengxin, Guo Pan. 2017. Discovery of Neoproterozoic A-type granite in northern Yangtze craton and its tectonic significance. *Earth Science*, 42(6): 957~973 (in Chinese with English abstract).
- Chappell B W. 1999. Aluminium saturation in I- and S-type granites and the characterization of fractionated haplogranites. *Lithos*, 46(3): 535~551.
- Chappell B W, White A J R. 1992. I-and S-type granites in the Lachlan fold belt. *Transactions of the Royal Society of Edinburgh Earth Sciences*, 83(1-2): 1~26.
- Chappell B W, White A J R. 1974. Two contrasting granite type. *Pacific Geology*, 8: 173~174.
- Chen Ling, Ma Changqian, She Zhenbing, Mason Roger, Zhang Jinyang, Zhang Chao. 2009. Petrogenesis and tectonic implications of A-type granites in the Dabie orogenic belt, China: Geochronological and geochemical constraints. *Geological Magazine*, 146(5): 638~651.
- Chen Ling, Ma Changqian, Zhang Jinyang, Liu Yuanyuan, She Zhenbing, Zhang Chao. 2012. The first geological map of intrusive rocks in Dabie orogenic belt and its adjacent areas and its explanatory notes. *Geological Bulletin of China*, 31(1): 13~19 (in Chinese with English abstract).
- Chen Wei, Xu Zhaowen, Li Hongchao, Yang Xiaonan, Chen Jinqua, Wang Hao, Wang Shaohua. 2013a. Petrogenesis and origin of the Xinxiang granitic batholith in Henan Province and its implication for the tectonic evolution of the western Dabie area. *Acta Geologica Sinica*, 87(10): 1510~1524 (in Chinese with English abstract).
- Chen Wei, Xu Zhaowen, Lu Xiancai, Yang Xiaonan, Li Hongchao, Qu Wenjun, Chen Jinquan, Wang Hao, Wang Shaohua. 2013b. Petrogenesis of the Ba'anzhai granite and associated Mo mineralization, western Dabie orogen, east-central China: Constraints from zircon U-Pb and molybdenite Re-Os dating, whole-rock geochemistry, and Sr-Nd-Pb-Hf isotopes. *International Geology Review*, 55: 1220~1238.
- Chen Wei, Xu Zhaowen, Qiu Wenhong, Li Chao, Yu Yang, Wang Hao, Yang Su. 2015. Petrogenesis of the Yaochong granite and Mo deposit, western Dabie orogen, eastern-central China: Constraints from zircon U-Pb and molybdenite Re-Os ages, whole-rock geochemistry and Sr-Nd-Pb-Hf isotopes. *Journal of Asian Earth Sciences*, 103: 198~211.
- Chen Wei, Xu Zhaowen, Chen Maohong, Yu Yang. 2016. Multiple sources for the origin of the early Cretaceous Xinxiang granitic batholith and its tectonic implications for the western Dabie orogen, eastern China. *Mineralogy and Petrology*, 110 (1): 29~41.
- Ding Li, Du Xiaoran, Zhou Shiquan. 2006. The Classification of Lava and Sedimentary Strata of late Mesozoic in the west part of Northern Dabie Orogenic Belt. *Geology & Mineral Resources of South China*, 22(2): 50~56 (in Chinese with English abstract).
- Du Jianguo, Zhang Peng. 1999. Mesozoic volcanic rocks in northern part of Dabie orogenic belt. *Geoscience*, 13(1): 57~65 (in Chinese with English abstract).
- Gao Xinyu, Zhao Taiping, Shi Xiaobin, Zhang Zhonghui, Bao Zhiwei. 2013. Geochemistry and petrogenesis of the Early Cretaceous Shangcheng and Daquandian granites in the North Dabie Mountains. *Geochimica*, 42(4): 307~339 (in Chinese with English abstract).
- Gao Shan, Zhang Benren, Jin Zhenmin, Kern H. 1999. Delamination of the lower Crust of the Qinling-Dabie orogenic belt. *Science in China (ser. D)*, 29 (6): 532~541 (in Chinese).
- Gao Yang, Mao Jingwen, Ye Huishou, Li Faling, Li Yongfeng, Luo Zhengzhan, Xiong Bikang, Meng Fang. 2014. Geochronology, geochemistry and Sr-Nd-Pb isotopic constraints on the origin of the Qian'echong porphyry Mo deposit, Dabie orogen, east China. *Journal of Asian Earth Sciences*, 85: 163~177.
- Hacker B R, Ratschbacher L, Webb L, Ireland T, Walker D, Dong S. 1998. U/Pb zircon ages constrain the architecture of the ultrahigh-pressure Qinling-Dabie orogen, China. *Earth and Planetary Science Letters*, 161(1-4): 215~230.
- He Yongsheng, Li Shuguang, Hoefs Jochen, Huang Fang, Liu Sheng-ao, Hou Zhenhui. 2007. Post-collisional granitoids from the Dabie orogen: New evidence for partial melting of a thickened continental crust. *Geochimica et Cosmochimica Acta*, 75: 3815~3838.
- Hu Zhaochu, Gao Shan, Liu Yongsheng, Hu Shenghong, Chen Haihong, Yuan Honglin. 2008. Signal enhancement in laser ablation ICP-MS by addition of nitrogen in the Central Channel gas. *Journal of Analytical Atomic Spectrometry*, 23 (8): 1093.
- Hu Zhaochu, Liu Yongsheng, Gao Shan, Liu Wengui, Zhang Wen, Tong Xirun, Lin Lin, Zong Keqing, Li Ming, Chen Haihong, Zhou Lian, Yang Lu, 2012a. Improved insitu Hf isotope ratio analysis of zircon using newly designed X skimmer cone and jet sample cone in combination with the addition of nitrogen by laser ablation multiple collector ICP-MS. *Journal of Analytical Atomic Spectrometry*, 27(9): 1391.
- Hu Zhaochu, Liu Yongsheng, Gao Shan, Xiao Shaoquan, Zhao Laishi, Günther Detlef, Li Ming, Zhang Wen, Zong Keqing, 2012b. A "wire" signal smoothing device for laser ablation inductively coupled plasma mass spectrometry analysis. *Spectrochimica Acta Part B: Atomic Spectroscopy*, 78: 50~57.
- Huang Fang, Li Shuguang, Dong Feng, Li Qili, Chen Fukun, Wang Ying, Yang Wei. 2007. Recycling of deeply subducted continental crust in the Dabie Mountains, central China. *Lithos*, 96: 151~169.
- Huang Jie, Zheng Yongfei, Zhao Zifu, Wu Yuanbao, Zhou Jianbo, Liu Xiaoming. 2006. Melting of subducted continent: Element and isotopic evidence for a genetic relationship between Neoproterozoic and Mesozoic granitoids in the Sulu orogen. *Chemical Geology*, 229(4): 227~256.
- Jahn Bor-ming, Wu Fuyuan, Lo Ching-hua, Tsai Chin-ho. 1999. Crust-mantle interaction induced by deep subduction of the continental crust: Geochemical and Sr-Nd isotopic evidence from post-collisional mafic-ultramafic intrusions of the northern Dabie complex, central China. *Chemical Geology*, 157: 119~146.
- Li Hailong, Song Chuanzhong, Liu Guotong, Li Jiajiao, Ren Shenlian, Zhang Yan, Wang Wei, Yang Fan, Li Zhenwei, Yuan Fang. 2017. Deformation and metamorphic characteristics of the Xinxiang-Hongan area of the West Dabie orogenic belt. *Scientia Geologica Sinica*, 52(2): 470~486 (in Chinese with English abstract).
- Li Hongchao, Xu Zhaowen, Lu Xiancai, Chen Wei, Qu, Wenjun, Fu Bin, Yang, Xiaonan, Yang Jie, Chen Jinquan. 2012. Constraints on the timing and origin of the Dayinjian intrusion and associated molybdenum mineralization at the western Dabie orogen, central China. *International Geology Review*, 54: 1579~1596.
- Li Xianhua, Li Wuxian, Li Zhengxiang. 2007. On the genetic classification and tectonic implications of the Early Yanshanian granitoids in the Nanling Range, South China. *Chinese Science Bulletin*, 52(9): 981~991 (in Chinese).
- Liew T C, Hofmann A W. 1988. Precambrian crustal components,

- plutonic associations, plate environment of the Hercynian fold belt of central Europe: Indications from a Nd and Sr isotopic study. Contributions to Mineralogy and Petrology, 98(2):129~138.
- Liu Huan, Lin Shoufa, Song Chuazhong. 2018. A uniform orogen-parallel extension system of the shear zones in the Tongbai-Dabie orogenic belt, central China. *Acta Geologica Sinica* (English edition), 92(2):556~567.
- Liu Xiaochun, Jahn Bor-Ming, Liu Dunyi, Dong Shuwen, Li Sanzhong. 2004. SHRIMP U-Pb zircon dating of a metagabbro and eclogites from western Dabieshan (Hong'an Block), China, and its tectonic implications. *Tectonophysics*, 394: 171~192.
- Liu Xiaochun, Dong Shuwen, Li Sanzhong, Xue Huaimin, Liu Jianmin, Qu Wei. 2005. Timing of the Hong'an Group in Hubei: Constraints from U-Pb dating of metagranitic intrusions. *Geology in China*, 32(1): 75~81 (in Chinese with English abstract).
- Liu Yifei, Jiang Sihong, Fang Donghui, Liu Yan. 2008. Zircon SHRIMP U-Pb dating of Laowan granite in Tongbai area, Henan Province, and its geological implications. *Acta Petrologica et Mineralogica*, 27(6): 33~37 (in Chinese with English abstract).
- Liu Yongsheng, Hu Zhaochu, Gao Shan, Günther Detlef, Xu Juan, Gao Changui, Chen Haihong. 2008. In situ analysis of major and trace elements of anhydrous minerals by LA-ICP-MS without applying an internal standard. *Chemical Geology*, 257 (1/2): 34~43.
- Liu Yongsheng, Gao Shan, Hu Zhaochu, Gao Changui, Zong Keqing, Wang Dongbing. 2010. Continental and oceanic crust recycling-induced melt-peridotite interactions in the Trans-North China orogen: U-Pb dating, Hf isotopes and trace elements in zircons from mantle xenoliths. *Journal of Petrology*, 51(1/2): 537~571.
- Ludwig K R. 2003. User's Manual for Isoplot 3.00: A Geochronological Toolkit for Microsoft Excel. Berkeley: No. 4. Berkeley Geochronology Center Special Publication, 39.
- Ma Changqian, Li Zhichang, Ehlers Carl, Yang Kunguang, Wang Renjing. 1998. A post-collisional magmatic plumbing system: Mesozoic granitoid plutons from the Dabieshan high-pressure and ultrahigh-pressure metamorphic zone, east-central China. *Lithos*, 45(1-4):431~456.
- Ma Changqian, Ehlers C, Xu Changhai, Li Zhichang, Yang Kunguang. 2000. The roots of the Dabieshan ultrahigh-pressure metamorphic terrane: constraints from geochemistry and Nd-Sr isotope systematics. *Precambrian Research*, 102: 279~301.
- Ma Changqian, Yang Kunguang, Ming Houli, Lin Guangchun. 2003. The timing of tectonic transition from compression to extension in Dabieshan: Evidence from Mesozoic granites. *Science in China Ser. D Earth Sciences* 33(9), 817~827.
- Meng Fang. 2013. Study on rock-forming and ore-forming of the Lingshan pluton in the northern margin of Dabie Mountains. PhD thesis of China University of Geosciences, Beijing (in Chinese with English abstract).
- Nair R, Chacko T. 2008. Role of oceanic plateaus in the initiation of subduction and origin of continental crust. *Geology*, 36: 583~586.
- Ratschbacher L, Hacker B R, Calvert A, Webb L E, Grimmer J C, McWilliams M O, Ireland T, Dong S, Hu J. 2003. Tectonics of the Qinling (central China): Tectonostratigraphy, geochronology, and deformation history. *Tectonophysics*, 366:1~53.
- Ren Jishun, Chen Tingyu, Niu Baogui, Liu Zhigang, Liu Fengren. 1990. *Tectonic Evolution of Continental Lithosphere and Ore-forming Beneath East China and Its Adjacent Areas*. Beijing: Science Press, 1~194 (in Chinese).
- Ren Zhi, Zhou Taofa, Yuan Feng, Zhang Dayu, Fan Yu, Fan Yu. 2014. The stages of magmatic system in Shapinggou molybdenum deposit district, Anhui Province: Evidence from geochronology and geochemistry. *Acta Petrologica Sinica*, 30 (4):1097~1116 (in Chinese with English abstract).
- Sun S S, McDonough W F. 1989. Chemical and isotopic systematics of oceanic basalts: implications for mantle composition and processes. *Geological Society London Special Publications*, 42 (1):313~345.
- Wan Jun, Wu Bo, Guo Pan, Liu Wanliang, Liu Chengxin. 2017. Zircon U-Pb dating and geochemical characteristics of the Xiadian magmatic rock body in western Dabie orogenic belt and its redefinition as the A-type granite. *Acta Petrologica et Mineralogica*, 36 (5): 633 ~ 645 (in Chinese with English abstract).
- Wang Chao, Zhao Zhan, Jiao Ruohong, Wang Xucheng, Xuanghai. 2010. Late-orogenic Granitoids (174~161 Ma) in the Dabie Orogenic Belt. *Geology & Mineral Resources of South China*, 26 (4): 8 ~ 15 (in Chinese with English abstract).
- Wang Chunyong, Zeng Rongsheng, Mooney W D, Hacker B R. 2000. A crustal model of the ultrahigh-pressure Dabie Shan orogenic belt, China, derived from deep seismic refraction profiling. *Journal of Geophysical Research Solid Earth*, 105 (B5):10857~10869.
- Wiedenbeck M, Allé P, Corfu F, Griffin W L, Meier M, Oberli F, Quadt Albrecht von, Roddick J C, Spiegel W. 1995. Threennatural zircon standards for U-Th-Pb, Lu-Hf, trace element and REE analyses. *Geostandards and Geoanalytical Research*, 19(1): 1~23.
- Wu Fuyuan, Li Xianhua, Yang Jinhui, Zheng Yongfei. 2007. Discussions on the petrogenesis of granites. *Acta Petrologica Sinica*, 23 (6): 1217 ~ 1238 (in Chinese with English abstract).
- Wu Fuyuan, Liu Xiaochi, Ji Weiqiang, Wang Jiamin, Yang Lei. 2017. Highly fractionated granites: Recognition and research. *Science China Earth Sciences*, 47(7):745~765 (in Chinese).
- Wu Yudong, Wang Zongqi, LiuChengxin, Jia Shaohua, Zhang Yutao, Wu Bo, Wang Gang. 2017. Zircon U-Pb age and geochemistry of the Fangfan A-type granite in western Dabie Mountains and their tectonic significance. *Acta Geologica Sinica*, 91(2):315~333 (in Chinese with English abstract).
- Wu Yuanbao, Zheng Yongfei. 2004. Genesis of zircon and its constraints on interpretation of U-Pb age. *Chinese Science Bulletin*, 49(16): 1589~1604 (in Chinese).
- Wu Yuanbao, Zheng Yongfei. 2013. Tectonic evolution of a composite collision orogen: An overview on the Qinling-Tongbai-Hong'an-Dabie-Sulu orogenic belt in central China. *Gondwana Research*, 23: 1402~1428.
- Xiong X L, Adam J, Green T H. 2005. Rutile stability and rutile/melt HFSE partitioning during partial melting of hydrous basalt: Implications for TTG genesis. *Chemical Geology*, 218: 339~359.
- Xu Changhai, Ma Changqian. 1998. Discussion on Mesozoic Magmatism and Metamorphic Transformation in Dabie block. *Geology & Mineral Resources of South China*, 6(2):16~23 (in Chinese with English abstract).
- Xu Haijin, Ma Changqian, Ye Kai. 2007. Early Cretaceous granitoids and their implications for the collapse of the Dabie orogen, eastern China: SHRIMP zircon U-Pb dating and geochemistry. *Chemical Geology*, 240(3): 238~259.
- Xu Haijin, Ye Kai, Ma Changqian. 2008. Early Cretaceous granitoids in the North Dabie and their tectonic implications: Sr-Nd and zircon Hf isotopic evidences. *Acta Petrologica Sinica*, 24:87~103 (in Chinese with English abstract).
- Xu Haijin, Ma Changqian, Zhang Junfeng, Ye Kai. 2013. Early Cretaceous low-Mg adakitic granites from the Dabie orogen, eastern China: Petrogenesis and implications for destruction of the over-thickened lower continental crust. *Gondwana Research*, 23: 190~207.
- Xu Shutong, Su Wen, Liu Yican, Jiang Laili, Ji Shouyuan, Okay A I, Sengor A M C. 1992. Diamond from the Dabie Shan

- metamorphic rocks and its implication for tectonic setting. *Science*, 256: 80~82.
- Xu Yixian, Zhang Sheng, Griffin W L, Yang Yingjie, Yang Bo, Luo Yinhe, Zhu Lupei, Afonso Juan Carlos, Lei Binghua. 2016. How did the Dabieorogen collapse? Insights from 3-D magnetotelluric imaging of profile data. *Journal of Geophysical Research*, 121(7): 5169~5185.
- Yang Meizhen, Zeng Jiannian, Tan Yongjun, Li Faling, Wan Shouquan. 2010. LA-ICP-MSzircon U-Pb and molybdenite Re-Os dating for Qian'echong porphyry-type Mo deposit in northern Dabie, China, and its geological significance. *Geological Science & Technology Information*, 29(5): 35~45 (in Chinese with English abstract).
- Yang Meizhen, Zeng Jiannian, Ren Aiqin, Wan Shouquan, Lu Jianpei. 2011. Identifying Characteristics of high Sulfidation-epithermal Huangcheng Shan silver deposit in Henan Province and their ore-search implication. *Geology and Exploration*, 47(6): 1059~1066 (in Chinese with English abstract).
- Yang Meizhen, Zeng Jiannian, Ren Aiqin, Lu Jianpei, Qin Yongjun, Li Faling. 2012. Geochemistry and zircon U-Pb geochronology of Mesozoic Shuangqiao volcanic rocks in the western segment of northern Dabie Mountain. *Acta Petrologica et Mineralogica*, 31(2): 133~144 (in Chinese with English abstract).
- Yang Meizhen, Lu Jianpei, Fu Jingjing, Ren Aiqin, Wang Shifeng. 2014. Magmatic hydrothermal gold and polymetallic metallogenesis related to Yanshanian magmatism of Laowan gold belt, Tongbai Mountain: Evidence from geochemistry, geochronology and ore-controlling structural geological constraints. *Mineral Deposits*, 33(3): 651~666 (in Chinese with English abstract).
- Yang Yongfei, Wang Pin, Chen Yanjing, Li Yi. 2017. Geochronology and geochemistry of the Tianmugou Mo deposit, Dabie Shan, eastern China: Implications for ore genesis and tectonic setting. *Ore Geology Reviews*, 81: 484~503.
- Yang Zeqiang, Tang Xiangwei. 2015. Geochemical characteristics and zircon LA-ICP-MS U-Pb isotopic dating of the Xiaofan rock bodies in North Dabieshan. *Acta Geologica Sinica*, 89(4): 692~700 (in Chinese with English abstract).
- Zhang Chao, Ma Changqian. 2008. Large-scale Late Mesozoic Magmatism in the Dabie Mountain: Constraints from zircon U-Pb dating and Hf isotopes. *Mineral. Petrol.*, 28(4): 71~79 (in Chinese with English abstract).
- Zhang Guowei, Zhang Benren, Yuan Xuecheng, Xiao Qinghui. 2001. Qinling Orogenic Belt and Continent Dynamics. Beijing: Science Press, 1~855 (in Chinese).
- Zhang Shaobing, Zheng Yongfei, Zhao Zifu, Wu Yuanbao, Yuan Honglin, Wu Fuyuan. 2009. Origin of TTG-like rocks from anatexis of ancient lower crust: Geochemical evidence from Neoproterozoic granitoids in South China. *Lithos*, 113: 347~368.
- Zhao Zifu, Zheng Yongfei, Wei Chunshen, Wu Yuanbao, Chen Fukun, Jahn Bor-ming. 2005. Zircon U-Pb age, element and C-O isotope geochemistry of post-collisional mafic-ultramafic rocks from the Dabie orogen in east-central China. *Lithos*, 83: 1~28.
- Zhao Zifu, Zheng Yongfei, Wei Chunshen, Wu Yuanbao. 2007. Post-collisional granitoids from the Dabie orogen in China: Zircon U-Pb age, element and O isotope evidence for recycling of subducted continental crust. *Lithos*, 93: 248~272.
- Zhao Zifu, Zheng Yongfei, Wei Chunshen, Chen Fukun. 2008. Zircon U-Pb ages, Hf and O isotopes constrain the crustal architecture of the ultrahigh-pressure Dabie orogen in China. *Chemical Geology*, 253: 222~242.
- Zhao Zifu, Zheng Yongfei. 2009. Remelting of subducted continental lithosphere, petrogenesis of Mesozoic magmatic rocks in the Dabie-Sulu orogenic belt. *Science in China (Ser. D-Earth Sci.)*, 52(9): 1295~1318.
- Zhou Hongsheng, Su Hua, Ma Changqian. 2009. Formation-age, tectonic setting and ascertainment of A-type granite on the Lingshan pluton in Dabie orogenic belt. *Journal of Xinyang Normal University*, 22(2): 222~226 (in Chinese with English abstract).
- Zhu Jiang, Wang Lianxun, Peng Sanguo, Peng Lianhong, Wu Cangxiong, Qiu Xiaofei. 2017. U-Pb zircon age, geochemical and isotopic characteristics of the Miaoya syenite and carbonatite complex, central China. *Geological Journal*, 52: 938~954.
- Zhu Jiang, Wu Changxiong, Peng Sanguo, Peng Lianhong, Zhang Chuang, Liu Jinming. 2018a. Geochronology and geochemistry of volcanic rocks from the Huangchengshan volcanogenic epithermal silver deposit, Dabieorogen, China: Implications for tectonic setting. *Earth Science*, 43(7): 2404~2419 (in Chinese with English abstract).
- Zhu Jiang, Wu Bo, Wang Lianxun, Peng Sanguo, Zhou Hanwen. 2018b. Neoproterozoic bimodal volcanic rocks and granites in the western Dabie area, northern margin of Yangtze block, China: implications for extension during the break-up of Rodinia. *International Geology Review*, DOI: 10.1080/00206814.2018.1512058.

参 考 文 献

- 曹正琦,蔡逸涛,曾佐勋,胡正祥,陈静,蒋幸福,孙政权,吴波,刘成新,郭盼. 2017. 扬子克拉通北缘新元古代A型花岗岩的发现及大地构造意义. *地球科学——中国地质大学学报*, 42(6): 957~973.
- 陈玲,马昌前,张金阳,刘园园,余振兵,张超. 2012. 首编大别造山带侵入岩地质图(1:50万)及其说明. *地质通报*, 31(1): 13~19.
- 陈伟,徐兆文,李红超,杨小男,陈进全,王浩,王少华. 2013a. 河南新县花岗岩岩基的岩石成因、来源及对西大别构造演化的启示. *地质学报*, 87(10): 1510~1524.
- 丁莉,杜晓冉,周世全. 2006. 大别造山带北缘西部中生代晚期火山、沉积地层的时代. *华南地质与矿产*, 22(2): 50~56.
- 杜建国,张鹏. 1999. 大别造山带北部的中生代火山岩. *现代地质*, 13(1): 57~65.
- 高山,张本仁,金振民, Kern H. 1999. 秦岭一大别造山带下地壳拆沉作用. *中国科学(D辑)*, 29(6): 532~541.
- 高昕宇,赵太平,施小斌,张忠慧,包志伟. 2013. 大别山北麓早白垩世商城和达权店岩体的地球化学特征与成因. *地球化学*, 42(4): 307~339.
- 李海龙,宋传中,刘国厅,李加好,任升莲,张妍,王微,杨帆,李振伟,袁芳. 2017. 西大别造山带中新县一红安地区的变质变形分析. *地质科学*, 52(2): 470~486.
- 李献华,李武显,李正祥. 2007. 再论南岭燕山早期花岗岩的成因类型与构造意义. *科学通报*, 52(9): 981~991.
- 刘晓春,董树文,李三忠,薛怀民,刘建民,曲玮. 2005. 湖北红安群的时代:变质花岗质侵入体U-Pb定年提供的制约. *中国地质*, 32(1): 75~81.
- 刘翼飞,江思宏,方东会,刘妍. 2008. 河南桐柏老湾花岗岩体锆石SHRIMP U-Pb年龄及其地质意义. *岩石矿物学杂志*, 27(6): 33~37.
- 马昌前,杨坤光,明厚利,林广春. 2003. 大别山中生代地壳从挤压转向伸展的时间:花岗岩的证据. *中国科学:地球科学*, 33(9): 817~827.
- 孟芳. 2013. 大别山北麓灵山岩体的成岩成矿作用研究. *中国地质大学(北京)博士学位论文*.
- 任纪舜,陈廷愚,牛宝贵,刘志刚,刘凤仁. 1990. 中国东部及邻区大陆岩石圈的构造演化与成矿. 北京:科学出版社, 1~194.
- 任志,周涛发,袁峰,张达玉,范裕,范羽. 2014. 安徽沙坪沟钼矿区中酸性侵入岩期次研究——年代学及岩石化学约束. *岩石学报*, 30(4): 1097~1116.
- 万俊,吴波,郭盼,刘万亮,刘成新. 2017. 西大别造山带夏店岩体锆石U-Pb年代学、地球化学特征及其A型花岗岩的厘定. *岩石矿物学杂志*, 36(5): 633~645.
- 王超,赵展,焦若鸿,王绪诚,许长海. 2010. 大别造山带晚造山期

- 花岗岩类. 华南地质与矿产, 26(4): 8~15.
- 吴福元, 李献华, 杨进辉, 郑永飞. 2007. 花岗岩成因研究的若干问题. 岩石学报, 23(6): 1217~1238.
- 吴福元, 刘小驰, 纪伟强, 王佳敏, 杨雷. 2017. 高分异花岗岩的识别与研究. 中国科学: 地球科学, 47(7): 745~765.
- 武昱东, 王宗起, 刘成新, 贾少华, 张玉涛, 吴波, 王刚. 2017. 西大别芳畈花岗岩锆石 U-Pb 年龄、地球化学特征及其构造意义. 地质学报, 91(2): 315~333.
- 吴元保, 郑永飞. 2004. 锆石成因矿物学研究及其对 U-Pb 年龄解释的制约. 科学通报, 49(16): 1589~1604.
- 许长海, 马昌前. 1998. 大别地块中生代岩浆作用—变质改造及其成因探讨. 华南地质与矿产, 6(2): 16~23.
- 续海金, 叶凯, 马昌前. 2008. 北大别早白垩纪花岗岩类 Sm-Nd 和锆石 Hf 同位素及其构造意义. 岩石学报, 24: 87~103.
- 杨梅珍, 曾键年, 覃永军, 李法岭, 万守权. 2010. 大别山北缘千鹅冲斑岩型钼矿床锆石 U-Pb 和辉钼矿 Re-Os 年代学及其地质意义. 地质科技情报, 29(5): 35~45.
- 杨梅珍, 曾键年, 任爱琴, 万守全, 陆建培. 2011. 河南省皇城山高硫化型浅成低温热液型银矿床识别特征及其找矿意义. 地质与勘探, 47(6): 1059~1066.
- 杨梅珍, 曾键年, 任爱琴, 陆建培, 覃永军, 李法岭. 2012. 大别山北缘西段双桥中生代火山岩地球化学及锆石 U-Pb 同位素年代学. 岩石矿物学杂志, 31(2): 133~144.
- 杨梅珍, 陆建培, 付静, 任爱琴, 王世峰. 2014. 桐柏山老湾金矿带与燕山期岩浆作用有关的岩浆热液金多金属矿床成矿作用——来自地球化学、年代学证据及控矿构造地质约束. 矿床地质, 33(3): 651~666.
- 杨泽强, 唐相伟. 2015. 北大别山肖畈岩体地球化学特征和锆石 LA-ICP-MS U-Pb 同位素定年. 地质学报, 89(4): 692~700.
- 张超, 马昌前. 2008. 大别山晚中生代巨量岩浆活动的启动: 花岗岩锆石 U-Pb 年龄和 Hf 同位素制约. 矿物岩石, 28(4): 71~79.
- 张国伟, 张本仁, 袁学诚, 肖庆辉. 2001. 秦岭造山带与大陆动力学. 北京: 科学出版社, 1~855.
- 周红军, 苏华, 马昌前. 2009. 灵山岩体的形成时代、构造背景及其 A 型花岗岩的厘定. 信阳师范学院学报: 自然科学版, 22(2): 222~226.
- 朱江, 吴昌雄, 彭三国, 彭练红, 张闯, 刘锦明. 2018a. 大别山皇城山银矿区及外围陈棚组火山岩 U-Pb 年代学、地球化学和成矿构造背景. 地球科学, 43(7): 2404~2419.

U-Pb zircon age, geochemistry and isotopic characteristics of the Tanchong and Chenchong granites in the western Dabie orogen, China: constraints on petrogenesis and timing of lower crustal delamination

ZHU Jiang^{* 1, 2)}, WU Cangxiong³⁾, PENG Sanguo^{1, 2)}, LIU Jinming³⁾, ZHANG Chuang³⁾, CHEN Qi⁴⁾

1) Wuhan Center, China Geological Survey, Wuhan, 430205; 2) Research Center of

Granitic Diagenesis and Mineralization, China Geological Survey, Wuhan, 430205; 3) Sixth Geological Brigade,

Hubei Geological Bureau, Xiaogan, Hubei, 432000; 4) China University of Geosciences, Wuhan, 430074

* Corresponding author: zhujiang.01@foxmail.com

Abstract

The Tanchong and Chenchong granitic stocks are situated in the northern margin of Xinxian batholith within the western Dabie orogen. They consist of monzogranite and granite porphyry, respectively. Elemental, whole-rock Sr-Nd and zircon U-Pb-Hf isotopic analyses have been carried out in this study, in order to understand their petrogenesis and tectonic significance. LA-ICP-MS zircon dating yields U-Pb ages of 133.5 ± 1.1 Ma and 132.9 ± 1.1 Ma for the Tanchong and Chenchong granites, respectively, indicating they formed in the early Cretaceous. These granites are characterized by high SiO_2 of 69.40% to 77.82%, Al_2O_3 of 11.72% to 15.26%, a total alkali of $\text{Na}_2\text{O} + \text{K}_2\text{O} = 6.40\%$ to 8.70% with $\text{K}_2\text{O}/\text{Na}_2\text{O} > 1$ and $\text{A/CNK} = 1.14$ to 1.66, and belong to the high-K calc-alkaline series. They are enriched in LREE with $(\text{La/Yb})_{\text{N}} = 22.98$ to 28.64 and unapparent Eu anomaly, and depleted in Ba, Nb, Ta, P, Ti and Y. They have moderate I_{Sr} values (0.707220 to 0.707557) and negative $\epsilon_{\text{Nd}}(t)$ values (-17.7 to -18.1), with two-stage Nd model ages of 2.36 to 2.40 Ga. Zircon $\epsilon_{\text{Hf}}(t)$ values are negative (-21.4 to -25.8) with an calculated two-stage Hf model ages of 2.24 to 2.48 Ga. Their petrographic and geochemical data suggest that the Tanchong and Chenchong granites are fractionated I-type granites, which are derived from partial melting of ancient crust of the Yangtze Block. Their equilibrated residues are probably garnet-bearing. We infer that the magmas of Tanchong and Chenchong stocks were formed in a thickened continental setting. Combining regional synchronous magmatic rocks, we propose that tectonic collapse of the western Dabie orogen probably started at about 133 Ma, which is consistent with the eastern Dabie orogen.

Key words: granite; geochronology; geochemistry; Sr-Nd-Hf isotopes; petrology; western Dabie orogen